FULLY COMPUTABLE A POSTERIORI ERROR ESTIMATOR USING ANISOTROPIC FLUX EQUILIBRATION ON ANISOTROPIC MESHES*

NATALIA KOPTEVA†

Abstract. Fully computable a posteriori error estimates in the energy norm are given for singularly perturbed semilinear reaction-diffusion equations posed in polygonal domains. Linear finite elements are considered on anisotropic triangulations. To deal with the latter, we employ anisotropic quadrature and explicit anisotropic flux reconstruction. Prior to the flux equilibration, divergence-free corrections are introduced for pairs of anisotropic triangles sharing a short edge. We also give an upper bound for the resulting estimator, in which the error constants are independent of the diameters and the aspect ratios of mesh elements, and of the small perturbation parameter.

Key words. a posteriori error estimate, anisotropic triangulation, anisotropic flux equilibration, flux reconstruction, anisotropic quadrature, energy norm, singular perturbation, reaction-diffusion.

AMS subject classifications. 65N15, 65N30.

1. Introduction. We consider linear finite element approximations to singularly perturbed semilinear reaction-diffusion equations of the form

$$Lu := -\varepsilon^2 \triangle u + f(x,y;u) = 0 \quad \text{for } (x,y) \in \Omega, \qquad u = 0 \quad \text{on } \partial\Omega, \tag{1.1}$$

posed in a, possibly non-Lipschitz, polygonal domain $\Omega \subset \mathbb{R}^2$. Here $0 < \varepsilon \leqslant 1$. We also assume that f is continuous on $\Omega \times \mathbb{R}$ and satisfies $f(\cdot;s) \in L_\infty(\Omega)$ for all $s \in \mathbb{R}$, and the one-sided Lipschitz condition $f(x,y;u) - f(x,y;v) \geqslant C_f[u-v]$ whenever $u \geqslant v$, with some constant $C_f \geqslant 0$. Then there is a unique $u \in W^2_\ell(\Omega) \subseteq W^1_q(\Omega) \subset C(\bar\Omega)$ for some $\ell > 1$ and $q > 2$ [9, Lemma 1]. We additionally assume that $C_f + \varepsilon^2 \geqslant 1$ (as a division by $C_f + \varepsilon^2$ immediately reduces (1.1) to this case).

Our goal is to give explicitly and fully computable a posteriori error estimates on reasonably general anisotropic meshes (such as on Fig. 2.1 and Fig. 2.2) in the energy norm defined by

$$|\!|\!| v |\!|\!|_{\varepsilon;\Omega} := \left\{ \varepsilon^2 \|\nabla v\|^2_\Omega + C_f \|v\|^2_\Omega \right\}^{1/2},$$

where $\|\cdot\|_{\mathcal{D}} := \|\cdot\|_{L_2(\mathcal{D})}$ $\forall \mathcal{D} \subseteq \Omega$. This goal is achieved by a certain combination of explicit flux reconstruction and flux equilibration.

Flux equilibration for equations of type (1.1) was considered in [1, 3, 4, 7] on shape-regular meshes (see also [2, Chap. 6] for the case $\varepsilon = 1$), and in [10] on anisotropic meshes. The estimators in [3, 4, 7] are based on flux reconstructions, while [1, 10] employ solutions of certain local problems.

Our approach in this paper differs from the previous work in a few ways.

- The fluxes are equilibrated within a local patch using anisotropic weights depending on the local, possibly anisotropic, mesh geometry (see (5.3)).
- Prior to the flux equilibration, divergence-free corrections are introduced for pairs of anisotropic triangles sharing a short edge (see §6, in particular, (6.2)).
- A certain anisotropic quadrature is used on anisotropic elements (see §3). This is motivated by some observations made in [13], and also enables us to drop some mesh assumptions made in recent papers [14, 15].

*The author was partially supported by Science Foundation Ireland grant SFI/12/IA/1683

†Department of Mathematics and Statistics, University of Limerick, Limerick, Ireland (natalia.kopteva@ul.ie).

- Our estimator is explicitly and fully computable in the sense that it involves no unknown error constants (unlike other estimators on anisotropic meshes, such as in [10, 14, 15]).
- In contrast to [10], an upper bound for our estimator involves no matching functions (which we discuss below). In fact, the error constant C in the upper bound (1.2) is independent not only of the diameters and the aspect ratios of mesh elements, but also of the small perturbation parameter ε.
- Unlike [1, 3, 4, 7], and also [23, 18, 20, 19], we consider the semilinear case, which mostly simplifies the presentation (as f may include a few linear terms).
- By contrast, dealing with anisotropic elements requires some non-incemental changes in the flux construction and also a more intricate analysis compared to the isotropic-mesh case.
- The efficiency of error estimators on anisotropic meshes was addressed in [18, 20, 19] using the standard bubble function approach. However, a numerical example will be given in §9 that clearly demonstrates that short-edge jump residual terms in such bounds are not sharp. So, under additional restrictions on the anisotropic mesh, we shall give a new bound for the short-edge jump residual terms, and thus show that at least for some anisotropic meshes the error estimator constructed in the paper is efficient.

The robustness of our estimator, denoted by $\mathcal{E}$, with respect to the mesh aspect ratios, as well as the small perturbation parameter ε, is demonstrated by the following upper bound (which follows from Theorems 4.1 and 4.3):

$$\mathcal{E} \leqslant C \Big\{ \sum_{z\in\mathcal{N}} \min\{1,\, \varepsilon h_z^{-1}\} \left\|\varepsilon J_z\right\|_{\omega_z}^2 + \sum_{z\in\mathcal{N}} \left\|\min\{1,\, h_z\varepsilon^{-1}\}\, f_h^I\right\|_{\omega_z}^2 + \left\|f_h - f_h^I\right\|_\Omega^2 + \sum_{T\in\mathcal{T}} \left\|\lambda_T \operatorname{osc}(f_h^I;T)\right\|_T^2 + \sum_{z\in\mathcal{N}_{\partial\Omega}^*} \left\|\lambda_T f_h(z)\right\|_{\omega_z}^2 \Big\}^{1/2}, \tag{1.2}$$

where C is independent of the diameters and the aspect ratios of elements in the triangulation $\mathcal{T}$, and of ε. Here $\mathcal{N}$ is the set of nodes in $\mathcal{T}$, and ω_z is the patch of elements surrounding any $z \in \mathcal{N}$, while J_z is the maximum within ω_z of the standard jump in the normal derivative of the computed solution u_h across an element edge, $f_h = f(\cdot; u_h)$ and f_h^I is its standard piecewise-linear Lagrange interpolant. We also use $\lambda_T = \min\{1,\, H_T\varepsilon^{-1}\}$, $H_T \simeq \operatorname{diam}(T)$, $h_T \simeq H_T^{-1}|T|$, and $h_z \simeq |\omega_z|/\operatorname{diam}(\omega_z)$ (and some notation defined in the final paragraph of this section). The boundary subset $\mathcal{N}_{\partial\Omega}^*$ of $\mathcal{N}$ is defined in (2.4).

To relate (1.2) to interpolation error bounds (as well as to possible adaptive-mesh construction strategies), note that $|J_z|$ may be interpreted as approximating the diameter of ω_z under the metric induced by the squared Hessian matrix of the exact solution (while f_h^I approximates $\varepsilon^2 \triangle u$). Note also that the right-hand side in (1.2) is similar to the estimator in the recent paper [15], and reduces, in the case of shape-regular meshes, to a version of the estimator given by [23].

Explicit residual-type a posteriori error estimates for problems of type (1.1) were also given in [23, 9] on shape-regular meshes, [22, 12, 6] on anisotropic tensor-product meshes, and [18, 20, 19, 14, 15, 16] on more general anisotropic meshes (for $\varepsilon = 1$ in [22, 18]). All these estimates are not fully guaranteed in the sense that they involve unknown error constants. (The cited papers deal with the energy norm, except for [6, 9, 12, 14] addressing the maximum norm.)

Note that the error constants in the estimators of [18, 19, 20] (as well as the upper bound for the estimator [10] that we already mentioned) involve the so-called

matching functions. The latter depend on the unknown error and take moderate values only when the grid is either isotropic, or, being anisotropic, is aligned correctly to the solution, while, in general, they may be as large as mesh aspect ratios. The presence of such matching functions in the estimator is clearly undesirable, and is entirely avoided in recent papers [14, 15, 16], as well as in our upper bound (1.2).

Finally, note that a posteriori error estimation on anisotropic meshes presents a more serious challenge not only compared to the shape-regular-mesh case, but also to the a priori error estimation. Indeed, there is a vast number of papers showing that a-priori-chosen anisotropic meshes offer an efficient way of computing reliable numerical approximations of solutions that exhibit sharp boundary and interior layers. In the context of singularly perturbed differential equations, such as (1.1) with $\varepsilon \ll 1$, see, for example, [8, 11, 17, 21] and references therein.

The paper is organized as follows. In §2, we list all triangulation assumptions. Next, §3 describes the considered finite element discretization with quadrature. The structure of the reconstructed flux and the main results are presented in §4. The case $h_z \lesssim \varepsilon$ is addressed in §§5–6, while §7 deals with the case $h_z \gtrsim \varepsilon$. The efficiency of the constructed estimator is illustrated by some numerical results in §8. We conclude the paper by discussing lower error bounds on anisotropic meshes in §9.

Notation. We write $a \simeq b$ when $a \lesssim b$ and $a \gtrsim b$, $a = \mathcal{O}(b)$ when $|a| \lesssim b$, and $a \lesssim b$ when $a \leqslant Cb$ with a generic constant C depending on Ω and f, but C does not depend on either ε or the diameters and the aspect ratios of elements in $\mathcal{T}$. Also, we write $a \ll b$ when $a < c_0 b$ with a fixed small constant c_0 (used to distinguish between anisotropic and isotropic elements). The indicator function $\mathbb{1}_A$ takes value 1 if condition A is satisfied, and vanishes otherwise. For any $\mathcal{D} \subset \Omega$, we let $\|\cdot\|_{\mathcal{D}} = \|\cdot\|_{L_2(\mathcal{D})}$, and $\operatorname{osc}(v;\mathcal{D}) = \sup_{\mathcal{D}} v - \inf_{\mathcal{D}} v \ \forall v \in L_\infty(\mathcal{D})$, while $\boldsymbol{\nu}$ and $\boldsymbol{\mu}$, possibly subscripted, denote the unit vectors on $\partial\mathcal{D}$ in the outward normal and counterclockwise tangential direction, respectively. For any triangles T and T' sharing an edge, a standard notation is used:

$$\big[\boldsymbol{\tau}\cdot\boldsymbol{\nu}\big]_{\partial T\cap\partial T'} := \boldsymbol{\tau}\cdot\boldsymbol{\nu}\big|_T + \boldsymbol{\tau}\cdot\boldsymbol{\nu}\big|_{T'}\,, \qquad \big[\partial_{\boldsymbol{\nu}} u_h\big]_{\partial T\cap\partial T'} := \big[\nabla u_h\cdot\boldsymbol{\nu}\big]_{\partial T\cap\partial T'}\,.$$

2. Triangulation assumptions. We shall use z, S and T to respectively denote particular mesh nodes, edges and triangular elements, while $\mathcal{N}$, $\mathcal{S}$ and $\mathcal{T}$ will respectively denote their sets. For each $T \in \mathcal{T}$, let H_T be the maximum edge length and $h_T := 2H_T^{-1}|T|$ be the minimum altitude in T. For each $z \in \mathcal{N}$, let ω_z be the patch of elements surrounding any $z \in \mathcal{N}$, $\mathcal{S}_z$ the set of edges originating at z, and

$$H_z := \operatorname{diam}(\omega_z), \quad h_z := \max_{T\subset\omega_z} h_T, \quad \mathring{h}_z := \min_{T\subset\omega_z} h_T, \quad \gamma_z := \mathcal{S}_z\backslash\partial\Omega. \tag{2.1}$$

(With slight abuse of notation, such as in the latter formula, we occasionally treat subsets of $\mathcal{N}$, $\mathcal{S}$ and $\mathcal{T}$ as sets of points.)

Throughout the paper we make some triangulation assumptions. All of them are automatically satisfied by shape-regular triangulations.

- *Maximum Angle condition.* Let the maximum interior angle in any triangle $T \in \mathcal{T}$ be uniformly bounded by some positive $\lambda_0 < \pi$.
- Let the number of triangles containing any node be uniformly bounded.
- For any $z \in \mathcal{N}$, one has

$$h_T \simeq \mathring{h}_z \ \text{ and } \ H_T \simeq H_z \qquad \text{or} \qquad h_T \simeq H_T \qquad \forall\ T \subset \omega_z. \tag{2.2}$$

We also distinguish subsets $\mathcal{N}_{\rm ani}$, $\mathcal{N}_{\rm iso}$ and $\mathcal{N}^*_{\partial\Omega}$ of $\mathcal{N}$ (see Fig. 2.2). Note that $\mathcal{N}_{\rm ani}\cap\mathcal{N}_{\rm iso}=\varnothing$, while $\mathcal{N}\backslash(\mathcal{N}_{\rm ani}\cup\mathcal{N}_{\rm iso})$ is not necessarily empty.

(1) *Anisotropic nodes*, whose set is denoted by $\mathcal{N}_{\rm ani}$, are such that

$$h_z \ll H_z, \qquad h_T \simeq h_z \ \text{ and } \ H_T \simeq H_z \quad \forall\ T\subset\omega_z. \tag{2.3}$$

Note that (2.3) implies (2.2), while $z\in\mathcal{N}_{\rm ani}$ implies $\mathring{h}_z\simeq h_z$.

(2) *Isotropic nodes*, to whose set we shall refer as $\mathcal{N}_{\rm iso}$, are such that $h_z\simeq H_z$.

(3) One may expect anisotropic elements near the boundary to be aligned along it. To distinguish some boundary nodes for which it is not the case, we introduce

$$\mathcal{N}^*_{\partial\Omega}:=\big\{z\in\mathcal{N}_{\rm ani}\cap\partial\Omega\backslash\{\text{corners of }\Omega\}\ \text{and}\ |\mathcal{S}_z\cap\partial\Omega|\simeq h_z\lesssim\varepsilon\big\}. \tag{2.4}$$

Occasionally, we shall make additional assumptions that we describe below.

$\mathcal{A}1$ Each $z\in\mathcal{N}$ with $h_z\lesssim\varepsilon$ satisfies $z\in\mathcal{N}_{\rm ani}\backslash\{\text{corners of }\Omega\}$ and condition $\mathcal{A}1_{\rm ani}$, or it satisfies condition $\mathcal{A}1_{\rm mix}$; see below.

$\mathcal{A}1_{\rm ani}$ *Quasi-non-obtuse anisotropic elements.* Let the maximum triangle angle at $z\in\mathcal{N}_{\rm ani}$ be bounded by $\frac{\pi}{2}+\lambda_1\frac{h_z}{H_z}$ for some positive constant λ_1.

$\mathcal{A}1_{\rm mix}$ With $\mathring{\mathcal{S}}_z:=\{S\subset\mathcal{S}_z:|S|\simeq\mathring{h}_z\}$ and $\mathring{\omega}_z:=\{T\subset\omega_z: h_T\simeq H_T\simeq\mathring{h}_z\}$ respectively denoting the sets of edges and isotropic triangles of diameter $\simeq\mathring{h}_z$ within ω_z, let $(\mathring{\omega}_z\cup\mathring{\mathcal{S}}_z)\backslash\{z\}$ be connected.

$\mathcal{A}2$ Each $z\in\mathcal{N}$ with $h_z\gtrsim\varepsilon$ satisfies $\mathring{h}_z\geqslant\sqrt{6}\varepsilon$.

Note that $\mathcal{A}1_{\rm ani}$ is always satisfied by isotropic elements, so it requires only some of the anisotropic part of the mesh to be close to a non-obtuse triangulation. $\mathcal{A}1_{\rm mix}$ is also always satisfied on shape-regular meshes (as then $\mathring{\omega}_z=\omega_z$). For anisotropic nodes, $\mathcal{A}1_{\rm mix}$ may be satisfied if $z\in\partial\Omega$ (in this case, $\mathring{\omega}_z=\varnothing$, while $\mathring{\mathcal{S}}_z\backslash\{z\}$ is connected only if $\mathring{\mathcal{S}}$ contains a single edge). Note also that $\mathcal{A}2$ is satisfied for any $z\notin\mathcal{N}_{\rm iso}$, while for isotropic nodes it does impose a mild restriction (as for the latter, $h_z\simeq H_z$, so whenever $H_z\gtrsim\varepsilon$, within ω_z we impose $h_T\geqslant\sqrt{6}\varepsilon$).

We shall also consider a weaker version of $\mathcal{A}1$.

$\mathcal{A}1^*$ Each $z\in\mathcal{N}$ with $h_z\lesssim\varepsilon$ satisfies $z\in\mathcal{N}_{\rm ani}\backslash\partial\Omega$ and condition $\mathcal{A}1^*_{\rm ani}$, or $z\in\mathcal{N}^*_{\partial\Omega}$ and satisfies $\mathcal{A}1_{\rm ani}$, or it satisfies condition $\mathcal{A}1_{\rm mix}$.

$\mathcal{A}1^*_{\rm ani}$ *Local Element Orientation condition.* For $z\in\mathcal{N}_{\rm ani}$, there exists a rectangle $R_z\supset\omega_z$ such that $|R_z|\simeq|\omega_z|$.

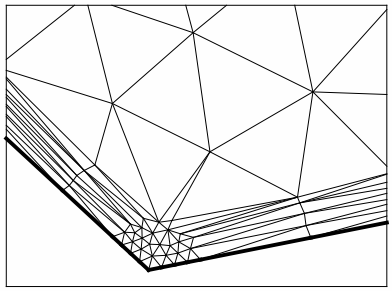

FIG. 2.1. *Example of a mesh that satisfies all assumptions made in §2 (including $\mathcal{A}1$ and $\mathcal{A}2$).*

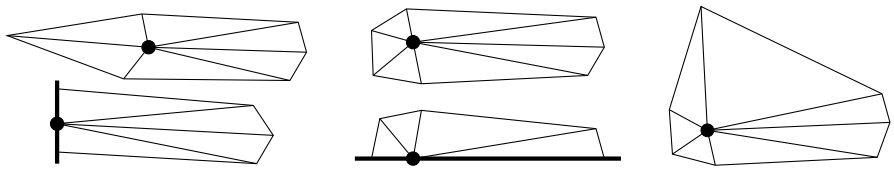

FIG. 2.2. *Examples of anisotropic nodes $z \in \mathcal{N}_{\rm ani}$ (left), nodes $z \in \mathcal{N}\backslash(\mathcal{N}_{\rm ani} \cup \mathcal{N}_{\rm iso})$ (centre), an isotropic node $z \in \mathcal{N}_{\rm iso}$ (right), and a node $z \in \mathcal{N}^*_{\partial\Omega}$ (bottom left). Examples of nodes that satisfy $\mathcal{A}1^*_{\rm ani}$ (top left), $\mathcal{A}1_{\rm ani}$ (bottom left), and $\mathcal{A}1_{\rm mix}$ (centre and right).*

3. Finite element method with quadrature. We discretize (1.1) using linear finite elements. Let $S_h \subset H^1_0(\Omega) \cap C(\bar\Omega)$ be a piecewise-linear finite element space relative to a triangulation $\mathcal{T}$, and let the computed solution $u_h \in S_h$ satisfy

$$\varepsilon^2\langle\nabla u_h, \nabla v_h\rangle + \langle f_h, v_h\rangle_h = 0 \quad \forall\ v_h \in S_h, \qquad\qquad f_h(\cdot) := f(\cdot; u_h). \tag{3.1}$$

Here $\langle\cdot,\cdot\rangle$ is the $L_2(\Omega)$ inner product, and $\langle\cdot,\cdot\rangle_h$ is its quadrature approximation.

We now describe $\langle f_h, v_h\rangle_h$ used in (3.1). For the integral over $T \in \mathcal{T}$, a quadrature formula Q_T is employed, which is anisotropic on a certain subset $\mathcal{T}^*$ of anisotropic elements:

$$Q_T(w) = |T| \sum_{j=1}^{3} \theta_{T;z_j} w(z_j) := \begin{cases} \frac{1}{3}|T|\big(w(z_1) + w(z_2) + w(z_3)\big) & \text{for } T \in \mathcal{T}\backslash\mathcal{T}^*, \\ \frac{1}{2}|T|\big(w(z_1) + w(z_2)\big) & \text{for } T \in \mathcal{T}^*. \end{cases} \tag{3.2}$$

Here $\{z_j\}_{j=1}^3$ are the vertices of T, with $z_3 =: z^*$ opposite the shortest edge, while

$$\mathcal{T}^* := \{T \in \mathcal{T} : h_T \ll H_T \text{ and } h_T \lesssim \varepsilon\} \setminus \mathcal{T}_0\,, \tag{3.3}$$

with $\mathcal{T}_0 \subset \{T \in \mathcal{T} : z^* \in \mathcal{N}_{\rm iso} \text{ and } z_1, z_2 \notin \mathcal{N}_{\rm ani}\backslash\partial\Omega\}$ (so, unless one wants to minimize $\mathcal{T}^*$, the simplest option is $\mathcal{T}_0 := \varnothing$). Now, let

$$\langle f_h, v_h\rangle_h := \sum_{T\in\mathcal{T}\backslash\mathcal{T}^*} Q_T(f_h v_h) + \sum_{T\in\mathcal{T}^*} Q_T(\bar f_h v_h), \tag{3.4}$$

where

$$\bar f_h = \bar f_{h;T} := \tfrac{1}{3}[f_h(z_1) + f_h(z_2) + f_h(z_3)] \quad \forall\ T \in \mathcal{T}. \tag{3.5}$$

As $\bar f_h$ is an elementwise constant approximation of f_h, so $Q_T(\bar f_h v_h) = \bar f_{h,T} Q_T(v_h)$.

Note that the discretization (3.1), (3.2), (3.3), (3.4) can be written as

$$\sum_{S\subset\gamma_z} \tfrac{1}{2}\varepsilon^2|S|\big[\partial_{\boldsymbol\nu} u_h\big]_S + \sum_{T\subset\omega_z} \theta_{T;z}|T|\, F_{T;z} = 0 \qquad \forall\ z \in \mathcal{N}\backslash\partial\Omega, \tag{3.6}$$

where $F_{T;z} := f_h(z)$ for $T \in \mathcal{T}\backslash\mathcal{T}^*$ and $F_{T;z} := \bar f_{h;T}$ for $T \in \mathcal{T}^*$. It will be sometimes convenient to replace the second sum here using an average $\bar F_z$ of $F_{T;z}$, associated with z, defined by

$$\bar F_z \sum_{T\subset\omega_z} \theta_{T;z}|T| := \sum_{T\subset\omega_z} \theta_{T;z}|T|\, F_{T;z} \ \ \forall\ z \notin \partial\Omega, \quad \bar F_z := \begin{cases} 0 & \text{for } z \in \mathcal{N}^*_{\partial\Omega} : H_z \gtrsim \varepsilon, \\ f_h(z) & \text{otherwise for } z \in \partial\Omega. \end{cases} \tag{3.7}$$

Remark 3.1. The above quadrature yields the standard linear lumped-mass finite element discretization on $\mathcal{T}\backslash\mathcal{T}^*$. On $\mathcal{T}^*$, a special anisotropic quadrature is employed (designed to address certain convergence issues reported in [13]). The resulting method may be also interpreted as the vertex-centered finite volume method (or the box method) with a special choice of control volumes, applied to the approximation of our equation $-\varepsilon^2\triangle u + f(\cdot;u) = 0$. A related interpretation as a Petrov-Galerkin method is also possible.

Remark 3.2. Our results remain valid, if $Q_T(f_h v_h)$ is replaced by $Q_T(\bar{f}_h v_h)$ in the first sum in (3.4)*. However, using $Q_T(f_h v_h)$ for $h_T \gg \varepsilon$ yields a superior discretization (as in this case the local stiffness matrices become negligible so diagonal mass matrices are preferable). On the other hand, replacing $Q_T(\bar{f}_h v_h)$ by $Q_T(f_h v_h)$ in the second sum in* (3.4) *yields a less standard lumped-mass discretization on $\mathcal{T}^*$. For the latter choice, our estimator will enjoy a version of the upper bound* (1.2) *with λ_T replaced by 1 whenever $h_T \ll H_T \lesssim \varepsilon$. Furthermore, all our results remain valid without any changes if $Q_T(\bar{f}_h v_h)$ is used only for $T \in \mathcal{T}^* : H_T \lesssim \varepsilon$.*

4. A posteriori error estimator. Main Results. We start with a relatively standard auxiliary result, a version of which can be found, for example, in [3, Lemma 1] and [7, Theorem 3.1].

THEOREM 4.1. *For any $u_h \in S_h$, let $\boldsymbol{\tau} \in H^1(\mathrm{div}, T)$ $\forall T \in \mathcal{T}$ also satisfy*

$$[\boldsymbol{\tau}\cdot\boldsymbol{\nu}] = [\partial_{\boldsymbol{\nu}} u_h] \qquad \text{on all } S \in \mathcal{S}\backslash\partial\Omega. \tag{4.1}$$

Then, for a solution u of (1.1)*, with $C_f > 0$, one has*

$$|\!|\!| u_h - u |\!|\!|_{\varepsilon;\Omega} \leqslant \mathcal{E} := \Big\{ \|\varepsilon\boldsymbol{\tau}\|_\Omega^2 + C_f^{-1}\|\varepsilon^2 \mathrm{div}\boldsymbol{\tau} + f_h\|_\Omega^2 \Big\}^{1/2}. \tag{4.2}$$

Proof. With $v := u_h - u$, one has

$$\begin{aligned} |\!|\!| u_h - u |\!|\!|_{\varepsilon;\Omega}^2 &\leqslant \varepsilon^2\langle\nabla(u_h-u), \nabla v\rangle + \langle f(\cdot;u_h) - f(\cdot;u), v\rangle \\ &= \varepsilon^2\langle\nabla u_h, \nabla v\rangle + \langle f(\cdot;u_h), v\rangle\,, \\ &= \varepsilon^2\langle\boldsymbol{\tau}, \nabla v\rangle + \langle\varepsilon^2\mathrm{div}\boldsymbol{\tau} + f_h, v\rangle, \end{aligned}$$

which immediately implies (4.2). Here we employed the observation (obtained using $\triangle u_h = 0$ in any T, and (4.1)) that

$$\langle\nabla u_h, \nabla v\rangle + \langle \underbrace{\triangle u_h}_{=0}, v\rangle = \sum_{S\in\mathcal{S}} \int_S v \underbrace{[\partial_{\boldsymbol{\nu}} u_h]}_{=[\boldsymbol{\tau}\cdot\boldsymbol{\nu}]} = \langle\boldsymbol{\tau}, \nabla v\rangle + \langle\mathrm{div}\boldsymbol{\tau}, v\rangle.$$

Note that here (as well as in (4.2)), with slight abuse of notation, we understood $\triangle u_h$ and $\mathrm{div}\boldsymbol{\tau}$ as regular functions in Ω defined elementwise. ∎

*Remark 4.2 (*Cases $C_f \geqslant 0$ and $C_f = C_f(x,y)$*). An inspection of the above proof shows that the estimator $\mathcal{E}$ in* (4.2) *can be replaced by a more general*

$$\mathcal{E} := \Big\{ (1-\vartheta)^{-1}\|\varepsilon\boldsymbol{\tau}\|_\Omega^2 + \big(C_f + \varepsilon^2 C_\Omega^{-2}\vartheta\big)^{-1}\|\varepsilon^2\mathrm{div}\boldsymbol{\tau} + f_h\|_\Omega^2 \Big\}^{1/2},$$

where C_Ω is the Poincaré constant, and $\vartheta \in [0,1)$ is an arbitrary constant, with $\vartheta > 0$ unless $C_f > 0$. Note also that if $C_f = C_f(x,y)$, the above result remains valid with an obvious modification of the energy norm to $|\!|\!| v |\!|\!|_{\varepsilon;\Omega} := \big\{\varepsilon^2\|\nabla v\|_\Omega^2 + \|C_f^{1/2} v\|_\Omega^2\big\}^{1/2}$ and a similar modification of $\mathcal{E}$.

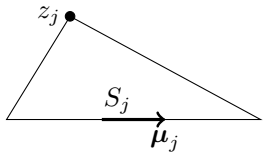

FIG. 4.1. *Notation used in* (4.6)*: the edge S_j is opposite to the vertex z_j, the counterclockwise tangential unit vector $\boldsymbol{\mu}_j$ lies along S_j.*

4.1. Structure of $\boldsymbol{\tau}$. Clearly, $\boldsymbol{\tau}$ that satisfies the conditions of Theorem 4.1 is not unique, and there are various choice available in the literature.

Our task in this paper is to explicitly define $\boldsymbol{\tau}$ to be used in (4.2) in a way that is appropriate for anisotropic meshes. We introduce a suitable $\boldsymbol{\tau}$ in the form

$$\boldsymbol{\tau} := \sum_{z\in\mathcal{N}} \boldsymbol{\tau}_z + \sum_{T\in\mathcal{T}^f} \boldsymbol{\tau}_T^f + \sum_{S\in\mathcal{S}^*} \boldsymbol{\tau}_S^J, \qquad \mathcal{T}^f := \{T\in\mathcal{T} : H_T \lesssim \varepsilon\}, \tag{4.3}$$

where $\boldsymbol{\tau}_z$, $\boldsymbol{\tau}_T^f$, and $\boldsymbol{\tau}_S^J$ have support on ω_z, T, and $T\cup T'$ for $S=\partial T\cap\partial T'$, respectively. It is also convenient to set $\boldsymbol{\tau}_T^f$ and $\boldsymbol{\tau}_S^J$ to 0 whenever respectively $T\notin\mathcal{T}^f$ and $S\notin\mathcal{S}^*$. Under condition $\mathcal{A}1$, we set $\mathcal{S}^*:=\varnothing$, while otherwise $\mathcal{S}^*$ is essentially the set of short edges shared by pairs of anisotropic triangles (see §6 for details).

To be more precise, in the case $\mathcal{S}^*=\varnothing$, the function $\boldsymbol{\tau}_z$, with support on ω_z, is simply required to satisfy

$$[\boldsymbol{\tau}_z\cdot\boldsymbol{\nu}] = \phi_z[\partial_{\boldsymbol{\nu}} u_h] \ \text{ on } \ \gamma_z, \qquad \boldsymbol{\tau}_z\cdot\boldsymbol{\nu} = 0 \ \text{ on } \ \partial\omega_z\backslash\partial\Omega, \tag{4.4}$$

where $\{\phi_z\}_{z\in\mathcal{N}}$ are the standard basis hat functions. The function $\boldsymbol{\tau}_T$, with support in T, satisfies

$$\boldsymbol{\tau}_T\cdot\boldsymbol{\nu} = 0 \quad \text{on } \partial T \quad \text{and} \quad \varepsilon^2 \mathrm{div}\boldsymbol{\tau}_T + (f_h^I - \bar{f}_h) = 0 \quad \text{in } T \qquad \forall\ T\in\mathcal{T}^f, \tag{4.5}$$

and is explicitly defined (see, e.g., [3, (22)]) by

$$\boldsymbol{\tau}_T^f := b_1\phi_2\phi_3|S_1|\boldsymbol{\mu}_1 + b_2\phi_3\phi_1|S_2|\boldsymbol{\mu}_2 + b_3\phi_1\phi_2|S_3|\boldsymbol{\mu}_3, \qquad b_j := \tfrac{1}{3}\varepsilon^{-2}\nabla f_h^I\cdot|S_j|\boldsymbol{\mu}_j\,, \tag{4.6}$$

where $\{z_j\}_{j=1}^3$ are the vertices of T with the corresponding basis functions $\phi_j:=\phi_{z_j}$, and for $j=1,2,3$, the edge S_j is opposite to z_j, while the counterclockwise tangential unit vector $\boldsymbol{\mu}_j$ lies along S_j; see Fig. 4.1.

4.2. Upper bound for the estimator. In this section, we present a theorem, which, combined with (4.2), gives the upper bound (1.2) for the estimator $\mathcal{E}$. At the same time, this theorem provides valuable information on the local properties of the components of $\boldsymbol{\tau}$ in (4.3). These components (except for $\boldsymbol{\tau}_T^f$) are constructed and analyzed in §§5–6 for the case $h_z\lesssim\varepsilon$, and in §7 for the case $h_z\gtrsim\varepsilon$. So, with the exception of (4.9), all bounds in the following theorem will be obtained in these forthcoming sections. (To be more precise, here we summarize the results of Lemmas 5.5, 5.6, 6.3 and 7.5.)

THEOREM 4.3. *Let u_h solve* (3.1) *with $\langle\cdot,\cdot\rangle_h$ defined in §3, and set*

$$J_z := \max_{S\subset\gamma_z}\Big|[\partial_{\boldsymbol{\nu}} u_h]_S\Big| \qquad \textit{and} \qquad \lambda_T := \min\{1,\, H_T\varepsilon^{-1}\} \quad \forall T\in\mathcal{T}.$$

(i) Under conditions $\mathcal{A}1$ and $\mathcal{A}2$, one can construct $\boldsymbol{\tau}$, subject to (4.1)*, in the form* (4.3) *with $\mathcal{S}^* = \varnothing$, where $\boldsymbol{\tau}_z$ and an associated function g_z, both with support in ω_z, satisfy, for any $z \in \mathcal{N}$,*

$$\sum_{\substack{z\in\mathcal{N}:\\ h_z\lesssim\varepsilon}} \varepsilon^2 \mathrm{div}\boldsymbol{\tau}_z + \bar{f}_h = \sum_{z\in\mathcal{N}} g_z \quad \text{in } \Omega, \tag{4.7}$$

$$\mathbb{1}_{h_z\gtrsim\varepsilon}\,\|\varepsilon^2\mathrm{div}\boldsymbol{\tau}_z\|_{\omega_z} + \|\varepsilon\boldsymbol{\tau}_z\|_{\omega_z} + \|g_z\|_{\omega_z} \lesssim \min\{1, \varepsilon h_z^{-1}\}^{1/2}\|\varepsilon J_z\|_{\omega_z} + \min\{1, h_z\varepsilon^{-1}\}\|f_h^I\|_{\omega_z}$$
$$+ \sum_{T\subset\omega_z} \lambda_T \|\mathrm{osc}(f_h^I; T)\|_T + \mathbb{1}_{z\in\mathcal{N}^*_{\partial\Omega}}\,\|\lambda_T f_h(z)\|_{\omega_z}, \tag{4.8}$$

while $\boldsymbol{\tau}_T^f$ from (4.6) *satisfies* (4.5)*, and, for any $T \in \mathcal{T}$,*

$$\|\varepsilon^2\mathrm{div}\boldsymbol{\tau}_T^f + (f_h - \bar{f}_h)\|_T + \|\varepsilon\boldsymbol{\tau}_T^f\|_T \lesssim \lambda_T\|\mathrm{osc}(f_h^I; T)\|_T + \|f_h - f_h^I\|_T. \tag{4.9}$$

(ii) Under conditions $\mathcal{A}1^*$ and $\mathcal{A}2$, one can construct $\boldsymbol{\tau}$, subject to (4.1)*, in the form* (4.3) *with $\mathcal{S}^* \neq \varnothing$, such that the above relations* (4.7), (4.8), (4.9) *hold true and, in addition, for any edge $S = \partial T \cap \partial T' \in \mathcal{S}^*$ with an endpoint z,*

$$\mathrm{div}\boldsymbol{\tau}_S^J = 0 \ \text{ in } T\cup T', \qquad \big\|\varepsilon\boldsymbol{\tau}_S^J\big\|_{T\cup T'} \lesssim \big\|\varepsilon[\partial_{\boldsymbol{\nu}} u_h]_S\big\|_{T\cup T'} \lesssim \min\{1,\, \varepsilon h_z^{-1}\}^{1/2}\|\varepsilon J_z\|_{\omega_z}\,. \tag{4.10}$$

Proof of (4.9). If $T \in \mathcal{T}^f$, so, by (4.3), $\lambda_T \simeq H_T\varepsilon^{-1}$, a calculation [3, §3.3] shows that (4.6) implies (4.5), while $|\gamma_j| \lesssim \varepsilon^{-2}\mathrm{osc}(f_h^I; T)$ yields $|\varepsilon\boldsymbol{\tau}_T^f| \lesssim H_T\varepsilon^{-1}\mathrm{osc}(f_h^I; T)$. The desired bound (4.9) for $T \in \mathcal{T}^f$ follows. Otherwise, i.e. if $T \notin \mathcal{T}^f$, so $\lambda_T \simeq 1$, one has $\boldsymbol{\tau}_T^f = 0$, while $|f_h - \bar{f}_h| \leqslant |f_h - f_h^I| + \mathrm{osc}(f_h^I; T)$, so we again get (4.9). □

Remark 4.4. Note that for $z \in \mathcal{N}^*_{\partial\Omega}$, the bound (4.8) *involves $\lambda_T|f_h(z)| \simeq \min\{\varepsilon^{-1}, H_z^{-1}\}\, H_z|f_h(z)|$, where $\varepsilon^{-2}H_z|f_h(z)|$ may be interpreted as the diameter of ω_z under the metric induced by the squared Hessian matrix of the exact solution at $z \in \partial\Omega$. Indeed, as $u = 0$ on $\partial\Omega$, the Hessian matrix involves only the normal derivatives, while $\varepsilon^{-2}f_h = \varepsilon^{-2}f(\cdot; 0) = \partial_{\boldsymbol{\nu}}^2 u$ on $\partial\Omega$; see also the definition of $\mathcal{N}^*_{\partial\Omega}$.*

5. Construction of $\boldsymbol{\tau}_z$ for $h_z \lesssim \varepsilon$ under condition $\mathcal{A}1$. Let the patch ω_z be formed by N_z triangles $\{T_i\}_{i=1}^{N_z} \subset \mathcal{T}$, numbered counterclockwise so that γ_z is formed by the edges $\partial T_{i-1} \cap \partial T_i$ for $i = 1, \ldots, N_z$ if $z \notin \partial\Omega$ (with the notation $T_0 := T_{N_z}$), and for $i = 2, \ldots, N_z$ if $z \in \partial\Omega$ (see Fig. 5.1 (left, centre)). For each $T_i \subset \omega_z$, let z be opposite to the edge denoted S_i, with the outward normal and the counterclockwise tangential unit vectors denoted $\boldsymbol{\nu}_i$ and $\boldsymbol{\mu}_i$ (see Fig. 5.1 (right)).

Define $\boldsymbol{\tau}_z$ associated with z by

$$\boldsymbol{\tau}_z := \phi_z\big(\alpha_i\boldsymbol{\nu}_i + \beta_i d_i^{-1}\boldsymbol{\mu}_i\big) \quad \forall\ T_i \subset \omega_z, \qquad d_i := 2|T_i|\,|S_i|^{-1}, \tag{5.1a}$$

where, using $F_{T;z}$ and $\bar{F}_z$ from (3.6), (3.7),

$$\alpha_i := \varepsilon^{-2} d_i \theta_{T_i;z}\widetilde{F}_{T_i;z}, \qquad \widetilde{F}_{T;z} := \begin{cases} \bar{F}_z & \text{if } H_z \gtrsim \varepsilon \text{ and } z \in \mathcal{N}_{\mathrm{ani}}, \\ F_{T;z} & \text{otherwise.} \end{cases} \tag{5.1b}$$

Here we require $\{\beta_i\}_{i=1}^{N_z}$ to satisfy

$$\beta_{i-1} - \beta_i + \alpha_{i-1}\boldsymbol{\nu}_{i-1}\cdot|S_{i-1}^+|\boldsymbol{\nu}_{i-1}^+ + \alpha_i\boldsymbol{\nu}_i\cdot|S_i^-|\boldsymbol{\nu}_i^- = |S_i^-|\big[\partial_{\boldsymbol{\nu}}u_h\big]_{\partial T_{i-1}\cap\partial T_i} \tag{5.1c}$$

for $i = 1, \ldots, N_z$ if $z \notin \partial\Omega$, and for $i = 2, \ldots, N_z$ if $z \in \partial\Omega$. We use the notation $S_i^\pm := \partial T_i \cap \partial T_{i\pm1}$, as well as $\boldsymbol{\nu}_i^\pm$ and $\boldsymbol{\mu}_i^\pm$ for the outward normal and the counterclockwise tangential unit vectors of the edge $S_i^\pm$ in triangle T_i (see Fig. 5.1 (right)).

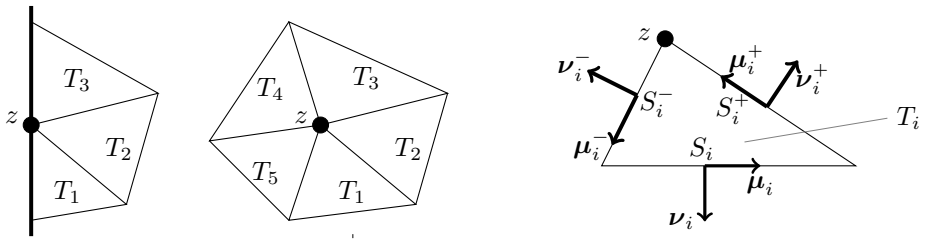

FIG. 5.1. *Notation in* (5.1)*: ω_z is formed by $\{T_i\}_{i=1}^{N_z}$ with $N_z = 3$ (left) and $N_z = 5$ (centre); the edge S_i in T_i is opposite to z, with the outward normal and the counterclockwise tangential unit vectors $\boldsymbol{\nu}_i$ and $\boldsymbol{\mu}_i$; the other edges $S_i^{\pm} = \partial T_i \cap \partial T_{i\pm1}$ have the outward normal and the counterclockwise tangential unit vectors $\boldsymbol{\nu}_i^{\pm}$ and $\boldsymbol{\mu}_i^{\pm}$ (right).*

LEMMA 5.1. *Let $h_z \lesssim \varepsilon$. Then relations* (5.1) *for $\boldsymbol{\tau}_z$ imply* (4.4) *and*

$$\varepsilon^2 \mathrm{div}\boldsymbol{\tau}_z + \theta_{T;z}\widetilde{F}_{T;z} = 0 \qquad \forall\ T \subset \omega_z, \tag{5.2a}$$

$$\|\varepsilon\boldsymbol{\tau}_z\|_{\omega_z} \lesssim \|h_z\varepsilon^{-1} f_h^I\|_{\omega_z} + \varepsilon \Big\{ \sum_{i=1}^{N_z} \beta_i^2 d_i^{-2} |T_i| \Big\}^{1/2}. \tag{5.2b}$$

The system (5.1c) *for $\{\beta_i\}_{i=1}^{N_z}$ is consistent and has infinitely many solutions.*

Proof. Combining $\mathrm{div}(\phi_z\boldsymbol{\mu}_i) = \nabla\phi_z \cdot \boldsymbol{\mu}_i = 0$ with $\mathrm{div}(\phi_z\boldsymbol{\nu}_i) = \nabla\phi_z \cdot \boldsymbol{\nu}_i = -d_i^{-1}$ one gets $\mathrm{div}\boldsymbol{\tau}_z + \alpha_i d_i^{-1} = 0$ in $T_i \subset \omega_z$, which immediately implies (5.2a). For (5.2b), note that $d_i\theta_{T_i;z} \lesssim h_z\theta_{T_i;z}$, because, in view of (3.2), (3.3), unless $d_i \lesssim h_z$, one has $T_i \in \mathcal{T}^*$ and $z = z_{T_i}^*$ so $\theta_{T_i;z} = 0$. Now, $|\varepsilon\alpha_i| \lesssim (h_z\varepsilon^{-1})\,\theta_{T_i;z}|\widetilde{F}_{T_i;z}|$. Combining this with (5.1b) and (3.7), one gets (5.2b)

Next, note that (4.4), combined with (5.1a), is equivalent to

$$\big(\alpha_{i-1}\boldsymbol{\nu}_{i-1} + \beta_{i-1}d_{i-1}^{-1}\boldsymbol{\mu}_{i-1}\big) \cdot \boldsymbol{\nu}_{i-1}^+ + \big(\alpha_i\boldsymbol{\nu}_i + \beta_i d_i^{-1}\boldsymbol{\mu}_i\big) \cdot \boldsymbol{\nu}_i^- = \big[\partial_{\boldsymbol{\nu}} u_h\big]_{\partial T_{i-1} \cap \partial T_i}.$$

Multiplying this by $|S_{i-1}^+| = |S_i^-|$ and noting that $d_i = \boldsymbol{\mu}_i \cdot |S_i^+|\boldsymbol{\nu}_i^+ = -\boldsymbol{\mu}_i \cdot |S_i^-|\boldsymbol{\nu}_i^-$, one gets (5.1c). So (5.1c) is, indeed, equivalent to (4.4).

Finally, consider the system (5.1c) for $\{\beta_i\}_{i=1}^{N_z}$. For this system to be consistent, it suffices to show that it is under-determined (as then, taking any specific β_1, one can uniquely compute all other $\{\beta_i\}$). For $z \in \partial\Omega$, there are $N_z - 1$ equations, so this system is clearly under-determined. For $z \notin \partial\Omega$, this is also the case as an application of $\sum_{i=1}^{N_z}$ to (5.1c) yields 0. To check the latter, one first employs the observation that $\boldsymbol{\nu}_i \cdot \big(|S_i^+|\boldsymbol{\nu}_i^+ + |S_i^-|\boldsymbol{\nu}_i^-\big) + 2|T_i|d_i^{-1} = 0$, and then recalls (5.1b), as well as (3.6) and (3.7). ∎

*Remark 5.2 (*Anisotropic flux equilibration*). The choice of a particular solution $\{\beta_i\}$ of* (5.1c) *is crucial, as our estimator, roughly speaking, involves the component $\sum_{i=1}^{N_z} \beta_i^2 d_i^{-2}|T_i|$ from* (5.2b)*, while, unless the mesh is shape-regular, $d_i^{-2}|T_i| = \frac{1}{4}|S_i|^2|T_i|^{-1}$ may vary very significantly within ω_z. One simple and useful approach is to minimize this component, i.e. given any particular solution $\{\hat{\beta}_i\}$ of* (5.1c)*, let*

$$\beta_i := \hat{\beta}_i - C_z, \qquad \textit{where} \quad \sum_i (\hat{\beta}_i - C_z) d_i^{-2}|T_i| = 0. \tag{5.3}$$

(Alternatively, one can set $\beta_i := 0$ for the element T_i with the largest $d_i^{-2}|T_i|$ within ω_z, or choose $\{\beta_i\}$ as in the proof of Lemma 5.6.)

FIG. 5.2. *Examples of nodes that satisfy* $\mathcal{A}1_{\rm mix}$ *with the set* $\{T_i\}_{i=1}^n$ *(used in the proof of Lemma 5.6) highlighted by the grey color:* $n=5$ *(top left),* $n=3$ *(bottom left),* $n=4$ *(right).*

*Remark 5.3 (*Computing $\boldsymbol{\tau}_z$ via optimization*). More generally, for* $h_z \lesssim \varepsilon$*, one can construct* $\boldsymbol{\tau}_z$ *using* (5.1a) *in which* $\{\alpha_i\}$ *and* $\{\beta_i\}$ *are chosen to minimize*

$$\sum_{i=1}^{N_z}\Big(\tfrac{1}{6}\varepsilon^2\alpha_i^2+\tfrac{1}{6}\varepsilon^2\beta_i^2 d_i^{-2}+[\theta_{T;z}F_{T;z}-\varepsilon^2\alpha_i d_i^{-1}]^2\Big)|T_i| \qquad \textit{subject to } (5.1c). \tag{5.4}$$

(Here we in fact minimize $\|\varepsilon\boldsymbol{\tau}_z\|_{\omega_z}^2+\|\varepsilon^2{\rm div}\boldsymbol{\tau}_z+\theta_{T;z}F_{T;z}\|_{\omega_z}^2$*, while* (5.1b) *is dropped). Then Theorem 4.3 remains valid (in view of the results in §§5.1–5.2 and §6).*

Remark 5.4. It is assumed throughout this section that any $z\in\mathcal{N}_{\rm ani}$ *with* $h_z\lesssim\varepsilon$ *also satisfies* $\omega_z\subset\mathcal{T}^*$*. This is consistent with the definition* (3.3) *of* $\mathcal{T}^*$ *as long as the somewhat imprecise condition* $h_T\lesssim\varepsilon$ *used in* (3.3) *always follows from* $h_z\lesssim\varepsilon$*.*

5.1. Proof of (4.7) **and** (4.8) **in Theorem 4.3(i) for** $h_z\lesssim\varepsilon$**.** Our findings in this section are presented as two lemmas.

LEMMA 5.5. *Let* $\{\boldsymbol{\tau}_z\}$ *satisfy* (5.1a), (5.1b) *for any* $z\in\mathcal{N}$ *with* $h_z\lesssim\varepsilon$*. Then for any* $z\in\mathcal{N}$*, there is a function* g_z *with support on* ω_z *that satisfies* (4.7) *and* (4.8)*.*

Proof. In any $T\subset\omega_z$, let $g_z:=\varepsilon^2{\rm div}\boldsymbol{\tau}_z+\theta_{T;z}F_{T;z}$ if $h_z\lesssim\varepsilon$, and $g_z:=\theta_{T;z}F_{T;z}$ otherwise. In view of (3.2), (3.6), $\sum_{\mathcal{N}\cap z\in\partial T}\theta_{T;z}F_{T;z}=\bar f_{h;T}=\bar f_h$ in any $T\in\mathcal{T}$, so the first assertion (4.7) follows. Next, if $h_z\gtrsim\varepsilon$, i.e. $\min\{1,\,h_z\varepsilon^{-1}\}\simeq 1$, one immediately gets $\|g_z\|_{\omega_z}\lesssim\min\{1,\,h_z\varepsilon^{-1}\}\|f_h^I\|_{\omega_z}$. Otherwise, i.e. if $h_z\lesssim\varepsilon$, a version of (5.2a) implies $g_z=\theta_{T;z}F_{T;z}-\varepsilon^2\alpha_i d_i^{-1}=\theta_{T;z}(F_{T;z}-\widetilde F_{T;z})$, and so $|g_z|\leqslant|F_{T;z}-\widetilde F_{T;z}|$ for any $T\subset\omega_z$. By (5.1b), unless $g_z=0$, one has $|g_z|\leqslant|F_{T;z}-\bar F_z|\leqslant{\rm osc}(f_h^I;\omega_z)+\mathbb{1}_{z\in\mathcal{N}_{\partial\Omega}^*}f_h(z)$, where we also used (3.7). At the same time, $H_z\gtrsim\varepsilon$ implies $1\simeq\min\{1,\,H_z\varepsilon^{-1}\}\simeq\lambda_T$ (as $z\in\mathcal{N}_{\rm ani}$ so $H_z\simeq H_T$). Combining these observations with $|T|\simeq|\omega_z|$ for any $T\subset\omega_z$ yields $\|g_z\|_{\omega_z}\lesssim$ the second line in (4.8). ∎

LEMMA 5.6. *Under condition* $\mathcal{A}1$*, for any* $z\in\mathcal{N}$ *with* $h_z\lesssim\varepsilon$*, there is a solution* $\{\beta_i\}_{i=1}^{N_z}$ *of* (5.1c) *such that* $\boldsymbol{\tau}_z$ *defined by* (5.1) *satisfies* (4.8)*.*

Proof. Our task is to show that $\|\varepsilon\boldsymbol{\tau}_z\|_{\omega_z}$ satisfies (4.8), in which the right-hand side involves $\min\{1,\,\varepsilon h_z^{-1}\}\simeq 1$ and $\min\{1,\,h_z\varepsilon^{-1}\}\simeq h_z\varepsilon^{-1}$. So it suffices to prove

$$\|\varepsilon\boldsymbol{\tau}_z\|_{\omega_z}\lesssim\|\varepsilon J_z\|_{\omega_z}+h_z\varepsilon^{-1}\|f_h^I\|_{\omega_z}+\sum_{T\subset\omega_z}\lambda_T\|{\rm osc}(f_h^I;T)\|_T+\mathbb{1}_{z\in\mathcal{N}_{\partial\Omega}^*}\|\lambda_T f_h(z)\|_{\omega_z}. \tag{5.5}$$

An inspection of the proof of Lemma 5.1 reveals that if $\widetilde F_{T;z}=F_{T;z}$ in (5.1b), then

$$\sum_{T_i\subset\omega_z}\|\varepsilon\alpha_i\|_{\omega_z}^2\lesssim|\omega_z|\,|h_z\varepsilon^{-1}f_h(z)|^2+|\omega_z|\sum_{\substack{T_i\in\mathcal{T}^*:\\ d_i\simeq h_{T_i}}}|d_i\varepsilon^{-1}\bar f_{h;T}|^2\lesssim\sum_{T\subset\omega_z}\|h_z\varepsilon^{-1}f_h^I\|_T^2,$$

where for the first relation we used (3.6) combined with (3.2), (3.3), and for the second, $|\omega_z|\simeq h_zH_z$ and $h_{T_i}H_z\simeq|T_i|$ for any $T_i\in\mathcal{T}^*$. One gets a similar conclusion for

the case $\widetilde{F}_{T;z} = \bar{F}_z$ in (5.1b) (in fact, the latter case is more straightforward as then $z \in \mathcal{N}_{\rm ani}$ so $|T_i| \simeq |\omega_z|$ for any $T_i \subset \omega_z$). Now, in view of (5.2b), to get the desired assertion (5.5), it suffices to show that

$$|\beta_i d_i^{-1}| \lesssim |J_z| + \max_{j=1,\dots,N_z} |\alpha_j| + |\hat{\sigma}_z|, \tag{5.6}$$

with some $\hat{\sigma}_z$ such that $\|\varepsilon\hat{\sigma}_z\|_{\omega_z}$ satisfies a version of (5.5).

For (5.6), we start with a straightforward observation that follows from (5.1c):

$$\text{if } \ |S_i^-| \simeq d_i \gtrsim d_{i-1} \quad \Rightarrow \quad |\beta_i d_i^{-1}| \lesssim |\beta_{i-1} d_{i-1}^{-1}| + |\alpha_{i-1}| + |\alpha_i| + |J_z|. \tag{5.7}$$

Consider three cases (a), (b) and (c).

(a) Suppose that z satisfies $\mathcal{A}_{\rm mix}$. Then the N_z triangles in ω_z can be numbered counterclockwise so that the set $\{T_i\}_{i=1}^n \neq \varnothing$, with some $n = n_z \leqslant N_z$, is formed by all triangles having at least one edge in $\mathring{S}_z$ (see Fig. 5.2). To be more precise, this set will include all triangles from $\mathring{\omega}_z$, and, possibly, one or two anisotropic triangles that either share an edge with $\mathring{\omega}_z \neq \varnothing$ or, if $\mathring{\omega}_z = \varnothing$ and so $\mathring{S}_z$ includes a single edge, touch this edge. Note that then $d_i \simeq \mathring{h}_z$ for $i = 1, \dots, n_z$ and $d_i \simeq H_z$ for $i > n_z$, while $|S_i^-| \simeq \mathring{h}_z$ for $i = 2, \dots, n_z$. So setting $\beta_1 := 0$ and applying (5.7) for $i > 1$, we arrive at (5.6) with $\hat{\sigma}_z := 0$.

(b) Next, consider $z \in \mathcal{N}_{\rm ani} \backslash \partial\Omega$ that satisfies $\mathcal{A}1_{\rm ani}$ (and so not $\mathcal{A}1_{\rm mix}$). Then $\mathring{\mathcal{S}}_z$ includes exactly two edges of length $\simeq \mathring{h}_z \simeq h_z$. Let the triangles $\{T_i\}_{i=1}^N$ forming the patch ω_z be numbered counterclockwise so that $\mathring{\mathcal{S}}_z = \{\partial T_{i-1} \cap \partial T_i\}_{i=1,m+1}$, for some $m = m_z \leqslant N_z - 2$ (see Fig. 5.3 (left)).

Note that $d_i \simeq h_z$ only for $i = 0, 1, m, m+1$ and $d_i \simeq H_z$ otherwise, while $|S_i^-| \simeq h_z$ for $i = 1, m$ and $\simeq H_z$ otherwise. Hence, one can employ (5.7) for $i \neq 0, m$. So it remains to get the desired bound (5.6) only for $i = 0, m$. For this, let

$$\widetilde{\sigma}_z := \sum_{i=2}^{m} |S_i^-| \big[\partial_{\boldsymbol{\nu}} u_h\big]_{\partial T_{i-1} \cap \partial T_i} + 2\varepsilon^{-2} \sum_{i=1}^{m} \theta_{T_i;z} |T_i| \, \widetilde{F}_{T_i;z} \tag{5.8}$$

(compare with (3.6)). Now, an application of $\sum_{i=1}^m$ to (5.1c) (and also noting that $\boldsymbol{\nu}_i \cdot \big(|S_i^+|\boldsymbol{\nu}_i^+ + |S_i^-|\boldsymbol{\nu}_i^-\big) + 2|T_i|d_i^{-1} = 0$) yields

$$\beta_0 - \beta_m + \alpha_0 \boldsymbol{\nu}_0 \cdot |S_0^+| \boldsymbol{\nu}_0^+ - \alpha_m \boldsymbol{\nu}_m \cdot |S_m^+| \boldsymbol{\nu}_m^+ = |S_1^-| \big[\partial_{\boldsymbol{\nu}} u_h\big]_{\partial T_0 \cap \partial T_1} + \widetilde{\sigma}_z. \tag{5.9}$$

So, for example, one can set $\beta_0 := 0$ and compute and then estimate β_m from (5.9). Or, one can choose β_0 and β_m, in agreement with (5.9), but in a more balanced way. Importantly, one can ensure for $i = 0, m$ that $|\beta_i d_i^{-1}| \lesssim |\alpha_i| + |J_z| + h_z^{-1}|\widetilde{\sigma}_z|$. Consequently, we get (5.6) for all i with $\hat{\sigma}_z := h_z^{-1}\widetilde{\sigma}_z$.

Finally, similarly to (3.7), define a version of (5.8):

$$\sigma_z := \sum_{i=2}^{m} |S_i^-| \big[\partial_{\boldsymbol{\nu}} u_h\big]_{\partial T_{i-1} \cap \partial T_i} + 2\varepsilon^{-2} \bar{F}_z \sum_{i=1}^{m} \theta_{T_i;z} |T_i|. \tag{5.10}$$

By (5.1b), unless $\widetilde{\sigma}_z = \sigma_z$, one has $\widetilde{F}_{T_i;z} \neq \bar{F}_z$ and so $H_z\varepsilon^{-1} \simeq \min\{1, H_z\varepsilon^{-1}\} \simeq \lambda_T$ (the latter is also because $z \in \mathcal{N}_{\rm ani}$), so $\varepsilon h_z^{-1}|\widetilde{\sigma}_z - \sigma_z| \lesssim \sum_{T \subset \omega_z} \lambda_T \operatorname{osc}(f_h^I; T)$. Combining this with a technical result (5.13) (obtained below in §5.2), one arrives at

$$|\varepsilon\hat{\sigma}_z| \lesssim |\varepsilon J_z| + h_z\varepsilon^{-1}|\bar{F}_z| + \sum_{T \subset \omega_z} \lambda_T \operatorname{osc}(f_h^I; T). \tag{5.11}$$

As $\|\bar{F}_z\|_{\omega_z} \lesssim \|f_h^I\|_{\omega_z}$ (by (3.6), (3.7)), so we have again obtained (5.6) with $\|\varepsilon\hat{\sigma}_z\|_{\omega_z}$ now satisfying a version of (5.5). This completes the proof of (5.5) for this case.

(c) It remains to consider $z \in \mathcal{N}^*_{\partial\Omega}$, which satisfies $\mathcal{A}1_{\rm ani}$ but not $\mathcal{A}1_{\rm mix}$. This case is similar to case (b), with a version of (5.9) becoming

$$\beta_1 - \beta_m - \alpha_1 \boldsymbol{\nu}_1 \cdot |S_1^-| \boldsymbol{\nu}_1^- - \alpha_m \boldsymbol{\nu}_m \cdot |S_m^+| \boldsymbol{\nu}_m^+ = \widetilde{\sigma}_z.$$

Again, using (5.13), we get a version of (5.11) with an additional term $H_z\varepsilon^{-1}|\bar{F}_z|$ in the right-hand side. As, by (3.7), unless $\bar{F}_z = 0$, one has $\bar{F}_z = f_h(z)$ and $H_z\varepsilon^{-1} \simeq \min\{1, H_z\varepsilon^{-1}\} \simeq \lambda_T$ for $z \in \mathcal{N}^*_{\partial\Omega}$, we again get (5.5). □

5.2. Estimation of σ_z. Here we give one technical result on σ_z. Throughout this section, we use the notation from the proof of Lemma 5.6.

LEMMA 5.7. *(i) If $z \in \mathcal{N}_{\rm ani}\backslash\partial\Omega$, with $h_z \lesssim \varepsilon$, satisfies $\mathcal{A}1^*_{\rm ani}$, then for σ_z of* (5.10) *one has*

$$\varepsilon h_z^{-1} \Big| \sigma_z - \sum_{i=1,m+1} \boldsymbol{\mu}_{i-1}^+ \cdot \mathbf{i}_\xi \, \frac{H_{T_{i-1}} H_{T_i}}{H_{T_{i-1}} + H_{T_i}} \, [\partial_{\boldsymbol{\nu}} u_h]_{\partial T_{i-1} \cap \partial T_i} \Big| \lesssim |\varepsilon J_z| + h_z \varepsilon^{-1} |\bar{F}_z|, \quad (5.12)$$

where $\mathbf{i}_\xi$ is the unit vector that points from z in the direction of any edge from $\{S_i^-\}_{i=2}^m$. (ii) If $z \in \mathcal{N}_{\rm ani}\backslash\{$corners of $\Omega\}$, with $h_z \lesssim \varepsilon$, satisfies $\mathcal{A}1_{\rm ani}$ but not $\mathcal{A}1_{\rm mix}$, then

$$\varepsilon h_z^{-1} |\sigma_z| \lesssim |\varepsilon J_z| + h_z \varepsilon^{-1} |\bar{F}_z| + \mathbb{1}_{z \in \mathcal{N}^*_{\partial\Omega}} \, H_z \varepsilon^{-1} |\bar{F}_z|. \quad (5.13)$$

Proof. (i) For any scalar w, let $[\![w]\!]_{\partial T_{i-1} \cap \partial T_i} := w\big|_{\partial T_i} - w\big|_{\partial T_{i-1}}$. Furthermore, for fixed $z \in \mathcal{N}$, introduce the local cartesian coordinates (ξ, η) such that $z = (0,0)$, and $\mathbf{i}_\xi$ points in the ξ direction (see Fig. 5.3 (left)). In these coordinates, let (ξ_i, η_i) be the endpoint of the edge $S_i^- = \partial T_{i-1} \cap \partial T_i$ on $\partial\omega_z$.

Now, a calculation shows that $|S_i^-| \big[\partial_{\boldsymbol{\nu}} u_h\big]_{\partial T_{i-1} \cap \partial T_i} = \eta_i [\![\partial_\xi u_h]\!] - \xi_i [\![\partial_\eta u_h]\!]$, where, by $\mathcal{A}^*_{\rm ani}$ and the maximum angle condition, any $|\eta_i| \lesssim h_z$, while $H_z^+ := \min\limits_{i=2,\dots m} \xi_i \simeq H_z$ and $0 \leqslant \xi_i - H_z^+ \lesssim h_z$, so

$$\sigma_z = -\sum_{i=2}^m H_z^+ [\![\partial_\eta u_h]\!]_{\partial T_{i-1} \cap \partial T_i} + \mathcal{O}(h_z |J_z|) + \varepsilon^{-2} \bar{F}_z \sum_{i=1,m} |T_i|. \quad (5.14)$$

Here we also used $\theta_{T_i;z} = 0$ for $i = 2, \dots, m-1$ and $\theta_{T_i;z} = \frac{1}{2}$ for $i = 1, m$ in view of $T_i \subset \mathcal{T}^*$ for any $T_i \subset \omega_z$ (see also (3.2), (3.3)).

Next, multiplying (3.6) combined with (3.7) by $2\varepsilon^{-2}$, then subtracting σ_z and applying a similar argument, one gets

$$-\sigma_z = \sum_{i=m+2}^N H_z^- [\![\partial_\eta u_h]\!]_{\partial T_{i-1} \cap \partial T_i} + \mathcal{O}(h_z |J_z|) + \varepsilon^{-2} \bar{F}_z \sum_{i=m+1,N} |T_i|. \quad (5.15)$$

Here $H_z^- := \min\limits_{i=m+2,\dots N} |\xi_i| \simeq H_z$, and we also used $|S_i^-| \simeq h_z$ for $i = 1, m+1$.

Finally, using $|T_1| = \frac{1}{2}|\xi_2\eta_1 - \xi_1\eta_2| = \frac{1}{2}\eta_1 H_z^+ + \mathcal{O}(h_z^2)$ (where $|\xi_1| + |\eta_2| \lesssim h_z$) and similar observations for the other triangle areas, we arrive at

$$\sum_{i=1,m} H_z^- |T_i| - \sum_{i=m+1,N} H_z^+ |T_i| = \mathcal{O}(h_z^2 H_z).$$

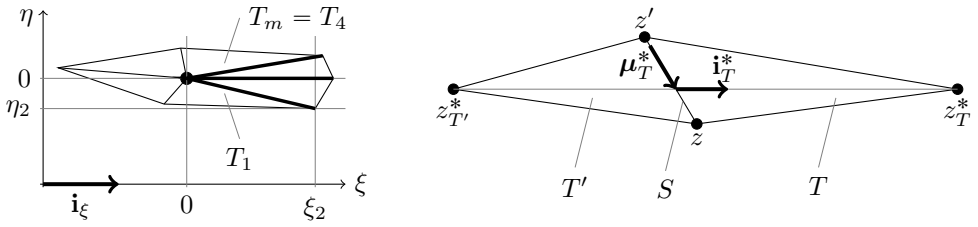

FIG. 5.3. *Notation used in Lemma 5.7 (left): the edges $\{S_i^-\}_{i=2}^m$ (here $m=4$) are highlighted, the unit vector $\mathbf{i}_\xi$ in the direction of any of these edges (here S_3^-), local coordinates (ξ,η), the endpoint (ξ_2,η_2) of the edge S_2^-. Notation used in the definition* (6.2) *of $\boldsymbol{\tau}_S^J$ (right).*

Combining this with (5.14), (5.15) and $\sum_{i=1}^N [\![\partial_\eta u_h]\!]_{\partial T_{i-1}\cap\partial T_i} = 0$ yields

$$(H_z^- + H_z^+)\sigma_z = \sum_{i=1,m+1} H_z^- H_z^+ \, [\![\partial_\eta u_h]\!]_{\partial T_{i-1}\cap\partial T_i} + h_z H_z \, \mathcal{O}\big(|J_z| + h_z\varepsilon^{-2}|\bar{F}_z|\big).$$

The desired assertion (5.12) follows in view of $H_z^+ = H_{T_i} + \mathcal{O}(h_z)$ for $i = 1, m$ and a similar relation with H_z^- for $i = m+1, N$, as well as

$$[\![\partial_\eta u_h]\!]_{\partial T_{i-1}\cap\partial T_i} = \boldsymbol{\mu}_{i-1}^+ \cdot \mathbf{i}_\xi \; [\partial_{\boldsymbol{\nu}} u_h]_{\partial T_{i-1}\cap\partial T_i}\,.$$

The latter follows from $\partial_\eta = \mathbf{i}_\eta\cdot\nabla$ combined with $[\![\nabla u_h]\!]_{\partial T_{i-1}\cap\partial T_i} = \boldsymbol{\nu}_i^- [\partial_{\boldsymbol{\nu}} u_h]_{\partial T_{i-1}\cap\partial T_i}$ and $\boldsymbol{\nu}_i^- \cdot \mathbf{i}_\eta = \boldsymbol{\mu}_{i-1}^+ \cdot \mathbf{i}_\xi$.

(ii) If $z \in \mathcal{N}_{\rm ani}\backslash\partial\Omega$, then $\mathcal{A}1$ implies $|\boldsymbol{\mu}_{i-1}^+ \cdot \mathbf{i}_\xi| \lesssim h_z H_z^{-1}$, so (5.12) implies (5.13). It remains to consider $z \in \mathcal{N}_{\partial\Omega}^*$. In view of $\mathcal{A}1$ and (2.4), one may choose the unit vector $\mathbf{i}_\xi$ in part (i) of this proof to be normal to $\partial\Omega$. As $u_h = \partial_\eta u_h = 0$ on $\partial\Omega$ so $\sum_{i=2}^m [\![\partial_\eta u_h]\!]_{\partial T_{i-1}\cap\partial T_i} = 0$, so (5.14) again yields the desired assertion (5.13). ☐

6. Construction of $\boldsymbol{\tau}_z$ for $h_z \lesssim \varepsilon$ under weaker condition $\mathcal{A}1^*$. Proof of Theorem 4.3(ii). This section deals with a weaker version $\mathcal{A}1^*$ of $\mathcal{A}1$. For this we need to address the terms subtracted from σ_z in (5.12) (which are $\lesssim h_z|J_z|$ under assumption $\mathcal{A}1$, but not under $\mathcal{A}1^*$).

Let $\mathcal{S}^* \subset \mathcal{S}$ in the definition (4.3) of $\boldsymbol{\tau}$ be

$$\mathcal{S}^* := \big\{S \text{ is shortest edge in } T \text{ and } T' :\; h_T \ll H_T,\; h_{T'} \ll H_{T'},\; h_T \simeq h_{T'} \lesssim \varepsilon\big\}. \quad (6.1)$$

Roughly speaking, $\mathcal{S}^* \subset \mathcal{S}$ is the set of short edges shared by pairs of anisotropic triangles. Now, we include a non-trivial component $\sum_{S\in\mathcal{S}^*} \boldsymbol{\tau}_S^J$ in $\boldsymbol{\tau}$, where $\boldsymbol{\tau}_S^J$ has support on $T\cup T'$ for any $S = \partial T\cap\partial T' \in \mathcal{S}^*$, and

$$\boldsymbol{\tau}_S^J := \kappa_S (d_T^*)^{-1}(\phi_z + \phi_{z'})\boldsymbol{\mu}_T^* \text{ in } T, \qquad \kappa_S := \boldsymbol{\mu}_T^* \cdot \mathbf{i}_T^* \, \frac{H_T H_{T'}}{H_T + H_{T'}} \, [\partial_{\boldsymbol{\nu}} u_h]_S\,. \quad (6.2)$$

Here $d_T^* := 2|T||S|^{-1}$, $\boldsymbol{\mu}_T^*$ is the tangential unit vector along S in the counterclockwise direction in T, the edge S joins the nodes z' and z, with $\boldsymbol{\mu}_T^*$ pointing from z' to z, and $\mathbf{i}_T^*$ is the unit vector in the direction from $z_{T'}^*$ to z_T^*, the latter being the vertices opposite to S in T' and T respectively; see Fig. 5.3 (right). Note that $\boldsymbol{\mu}_T^* = -\boldsymbol{\mu}_{T'}^*$ and $\mathbf{i}_T^* = -\mathbf{i}_{T'}^*$ so the definition of κ_S is consistent for T and T'.

LEMMA 6.1. *For any $S = \partial T \cap \partial T' \in \mathcal{S}^*$ with the notation* (6.1), (6.2), *one has* (4.10) *and*

$$\boldsymbol{\tau}_S^J \cdot \boldsymbol{\nu} = 0 \ \text{ on } S, \qquad |S''| \boldsymbol{\tau}_S^J \cdot \boldsymbol{\nu} = \kappa_S(\phi_z - \phi_{z'}) \ \text{ on any edge } S'' \subset \partial T \backslash S. \tag{6.3}$$

Proof. For $\mathrm{div}\boldsymbol{\tau}_S^J = 0$ in (4.10), as well as (6.3), imitate the proof of Lemma 5.1. For the first bound on $\varepsilon\boldsymbol{\tau}_S^J$ in (4.10), note that $d_T^* \simeq d_{T'}^* \simeq H_T$ implies $|\boldsymbol{\tau}_S^J| \lesssim H_T^{-1}|\kappa_S| \lesssim |[\partial_{\boldsymbol{\nu}} u_h]_S|$. For the final assertion in (4.10), note that $|T \cup T'||\omega_z|^{-1} \lesssim (h_T + h_{T'})h_z^{-1} \lesssim \min\{1, \varepsilon h_z^{-1}\}$. ☐

Now that $\sum_{S \in \mathcal{S}^*} \boldsymbol{\tau}_S^J$ is included in $\boldsymbol{\tau}$, we need to ensure that $\boldsymbol{\tau}$ still satisfies (4.1). For this, the definition of $\boldsymbol{\tau}_z$ should be updated to take into account the possibly non-trivial jumps $[\boldsymbol{\tau}_S^J \cdot \boldsymbol{\nu}]$ across γ_z. For a possible modification of $\boldsymbol{\tau}_z$ in the case $h_z \gtrsim \varepsilon$, see Remark 7.4.

For $h_z \lesssim \varepsilon$, the definition (5.1) of $\boldsymbol{\tau}_z$ is tweaked as follows. Relations (5.1a) and (5.1b) remain unchanged, while in (5.1c) we replace $\{\beta_i\}_{i=1}^{N_z}$ by $\{\beta_i^*\}_{i=1}^{N_z}$, where

$$\beta_i := \beta_i^* + \kappa_i + \kappa_{i+1}, \qquad \kappa_i := \begin{cases} \kappa_{\partial T_{i-1} \cap \partial T_i} & \text{if } \ \partial T_{i-1} \cap \partial T_i \subset \mathcal{S}^*, \\ 0 & \text{otherwise.} \end{cases} \tag{6.4}$$

*Remark 6.2 (*Anisotropic flux equilibration*). The observations of Remark 5.2 remain valid (although a version of system* (5.1c) *is now solved for $\{\beta_i^*\}$). One can simply use* (5.3) *(or choose $\{\beta_i\}$ as in the proof of Lemma 6.3).*

LEMMA 6.3. *Under condition $\mathcal{A}1^*$, for any $z \in \mathcal{N}$ with $h_z \lesssim \varepsilon$, let $\boldsymbol{\tau}_z$ be defined by* (5.1a) *and* (5.1b) *and use the notation* (6.1), (6.2). *Then there is a solution of the system* (5.1c), *in which $\{\beta_i\}_{i=1}^{N_z}$ is replaced by $\{\beta_i^*\}_{i=1}^{N_z}$ of* (6.4), *such that $\boldsymbol{\tau}$ of* (4.3) *satisfies* (4.1) *and the results of Lemmas 5.1, 5.5 and 5.6 remain true.*

Proof. One can easily check that, indeed, the results of Lemmas 5.1 and 5.5 remain true, while for Lemma 5.6, it suffices to obtain (5.6). That the normal jumps in $\boldsymbol{\tau}$ satisfy (4.1) can be checked by a direct calculation using (6.3) and taking into account that if $(\partial T_{i-1} \cap \partial T_i) \subset (\gamma_z \cap \mathcal{S}^*)$, then $\beta_i - \beta_{i-1} = \beta_i^* - \beta_{i-1}^*$ (in view of $\kappa_{i-1} = \kappa_{i+1} = 0$). Note that in the latter case (5.7) is still true.

Otherwise, i.e. for $(\partial T_{i-1} \cap \partial T_i) \notin (\gamma_z \cap \mathcal{S}^*)$, a version of (5.7) will be employed:

$$\text{if } |S_i^-| \simeq d_i \gtrsim d_{i-1} \ \Rightarrow \ |\beta_i d_i^{-1}| \lesssim |\beta_{i-1} d_{i-1}^{-1}| + \max_j |\alpha_j| + \max_j |\kappa_j| d_i^{-1} + |J_z|. \tag{6.5}$$

Next, consider two cases (a) and (b), as in the proof of Lemma 5.6, to get the bound (5.6) for $\beta_i d_i^{-1}$ and thus complete the proof.

(a) Suppose that z satisfies $\mathcal{A}_{\mathrm{mix}}$. Unless $\gamma_z \cap \mathcal{S}^* = \varnothing$ (and so the results of Lemma 5.6 apply), $\mathring{\omega}_z = \varnothing$ and $\mathring{\mathcal{S}}_z = \gamma_z \cap \mathcal{S}^*$ contains exactly one edge $\partial T_1 \cap \partial T_2$. Then note that $\kappa_i = 0$ unless $i = 2$. Set $\beta_1 := 0$ and use (5.7) with $i = 2$ as in the proof of Lemma 5.6. For $i > 2$, use (6.5), where $d_i \simeq H_z$, so the additional term $\max |\kappa_j| d_i^{-1} = |\kappa_2| H_z^{-1} \lesssim |J_z|$. So we get (5.6) with $\hat{\sigma}_z := 0$.

(b) It remains to consider $z \in \mathcal{N}_{\mathrm{ani}} \backslash \partial\Omega$ under condition $\mathcal{A}1_{\mathrm{ani}}^*$ (as $z \in \mathcal{N}_{\mathrm{ani}} \cap \partial\Omega$ satisfies either $\mathcal{A}1_{\mathrm{ani}}$ or $\mathcal{A}1_{\mathrm{mixed}}$, so have been considered in part (a) or in Lemma 5.6). We shall imitate part (b) from the proof of Lemma 5.6. Note that $(\partial T_{i-1} \cap \partial T_i) \subset (\gamma_z \cap \mathcal{S}^*)$ (and so $\kappa_i \neq 0$) only for $i = 1, m+1$. Hence, we employ (5.7) for $i = 1, m+1$,

FIG. 7.1. *Notation used in Lemma 7.1: each triangle $T^{\pm}\subset T$ shares the edge $S_T^{\pm}$ with T and has another edge of length $\varepsilon'\simeq\varepsilon$ along $S_T^{\mp}$.*

and (6.5) with $d_i \simeq H_z$ for $i \neq 1, m, m+1, N$, and it remains to bound $\beta_i d_i^{-1}$ for $i = 0, m$. For the latter, combining (5.9) with (6.4) yields

$$[\beta_0 - \kappa_1] - [\beta_m - \kappa_{m+1}] = \widetilde{\sigma}_z + \mathcal{O}\big(h_z|J_z|\big).$$

From this bound, one gets (5.6) only now $\hat{\sigma}_z := h_z^{-1}(\widetilde{\sigma}_z + \kappa_1 - \kappa_{m+1})$. As $|\widetilde{\sigma}_z - \sigma_z|$ was bounded in the proof of Lemma 5.6, to complete the proof, it remains to show

$$\varepsilon h_z^{-1}|\sigma_z + \kappa_1 - \kappa_{m+1}| \lesssim |\varepsilon J_z|.$$

The above follows from (5.12) using the following observations. For $\kappa_1 = \kappa_{\partial T_0\cap\partial T_1}$, we use the triangle T_0 with $\boldsymbol{\mu}^*_{T_0} = \boldsymbol{\mu}_0^+$ and $|\mathbf{i}^*_{T_0} + \mathbf{i}_\xi| \lesssim h_z H_z^{-1}$. Similarly, for $\kappa_{m+1} = \kappa_{\partial T_m\cap\partial T_{m+1}}$, we use the triangle T_m with $\boldsymbol{\mu}^*_{T_m} = \boldsymbol{\mu}_m^+$ and $|\mathbf{i}^*_{T_m} - \mathbf{i}_\xi| \lesssim h_z H_z^{-1}$. ∎

7. Construction of $\boldsymbol{\tau}_z$ for $h_z \gtrsim \varepsilon$ under condition $\mathcal{A}2$. Throughout this section, for any $T \subset \omega_z$, we use S_T, $\boldsymbol{\nu}_T$ and $\boldsymbol{\mu}_T$, as well as $S_T^{\pm}$, $\boldsymbol{\nu}_T^{\pm}$ and $\boldsymbol{\mu}_T^{\pm}$, defined as in §5 (see Fig. 5.1 (right)) only with subscript T in place of i when dealing with element T. We start with two useful technical results.

LEMMA 7.1. *Let $h_T \geqslant \sqrt{6}\varepsilon$. For any triangle T with a vertex z, there exist two functions $\boldsymbol{\tau}^+_{z;T}$ and $\boldsymbol{\tau}^-_{z;T}$ in T such that*

$$\boldsymbol{\tau}^{\pm}_{z;T}\cdot\boldsymbol{\nu} = 0 \ \text{ on } \partial T\backslash S_T^{\pm}, \qquad \boldsymbol{\tau}^{\pm}_{z;T}\cdot\boldsymbol{\nu} = \phi_z \ \text{ on } S_T^{\pm}, \tag{7.1a}$$

$$\|\varepsilon\,\mathrm{div}\boldsymbol{\tau}^{\pm}_{z;T}\|_T^2 = \|\boldsymbol{\tau}^{\pm}_{z;T}\|_T^2 = \tfrac{1}{2\sqrt{6}}\varepsilon|S_T^{\pm}|\varsigma_{T;z}^{-1}, \qquad \varsigma_{z;T} := \sin\angle(S_T^-, S_T^+). \tag{7.1b}$$

Proof. Let $\varepsilon' := \sqrt{6}\varepsilon$ and, skipping the subscripts when there is no ambiguity, set

$$\boldsymbol{\tau}^+ := -\varsigma^{-1}\varphi_z^+\boldsymbol{\mu}^-, \qquad \boldsymbol{\tau}^- := \varsigma^{-1}\varphi_z^-\boldsymbol{\mu}^+.$$

Here φ_z^+ is a barycentric coordinate in the triangle T^+ formed by the edge $S_T^+ = S^+$ and the point $z + \varepsilon'\boldsymbol{\mu}^-$ such that $\varphi_z^+\big|_z = 1$; see Fig. 7.1. Similarly, φ_z^- is a barycentric coordinate in the triangle T^- formed by the edge $S_T^- = S^-$ and the point $z - \varepsilon'\boldsymbol{\mu}^+$.

The boundary properties (7.1a) are satisfied as $\boldsymbol{\mu}^{\pm}\cdot\boldsymbol{\nu}^{\pm} = 0$ and $\varsigma = -\boldsymbol{\mu}^-\cdot\boldsymbol{\nu}^+ = \boldsymbol{\mu}^+\cdot\boldsymbol{\nu}^-$. Next, using $|T^+| = \frac{1}{2}\varepsilon'|S^+|\varsigma$,

$$\|\boldsymbol{\tau}^+\|_T^2 = \tfrac{1}{6}\varsigma^{-2}|T^+| = \tfrac{1}{2\sqrt{6}}\varepsilon\varsigma^{-1}|S^+|,$$

while $\mathrm{div}\boldsymbol{\tau}^+ = -\varsigma^{-1}\partial_{\boldsymbol{\mu}^-}\varphi_z^+ = \varsigma^{-1}\varepsilon'^{-1}$ so $\|\varepsilon\,\mathrm{div}\boldsymbol{\tau}^+\|_T^2 = (\varepsilon/\varepsilon')^2\varsigma^{-2}|T^+| = \|\boldsymbol{\tau}^+\|_T^2$. ∎

*Remark 7.2 (*Version of $\mathcal{A}2$*). In $\mathcal{A}2$, one can impose that each $z\in\mathcal{N}$ with $h_z \gtrsim \varepsilon$ satisfies $\mathring{h}_z \geqslant c'\varepsilon$ for any fixed positive constant c' (rather than $\mathring{h}_z \geqslant \sqrt{6}\varepsilon$). For this case, one can employ a version of the above lemma under the condition $h_T \geqslant c'\varepsilon$. Choosing $\varepsilon' := c'\varepsilon$ in the proof, one, indeed, arrives at the following version of* (7.1b)*:*

$$\|\varepsilon\,\mathrm{div}\boldsymbol{\tau}^{\pm}_{z;T}\|_T^2 = 6c'^{-2}\|\boldsymbol{\tau}^{\pm}_{z;T}\|_T^2 = (2c')^{-1}\varepsilon|S_T^{\pm}|\varsigma_{T;z}^{-1}\,.$$

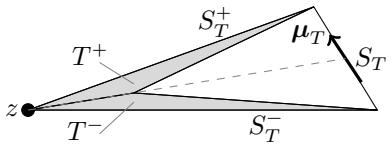

FIG. 7.2. *Notation used in Lemma 7.3: each triangle $T^\pm \subset T$ is formed by the edge $S_T^\pm$ and a common vertex lying on the median of T originating at z.*

LEMMA 7.3. *For any triangle T with a vertex z and its opposite edge S_T satisfying $|S_T| > 4\sqrt{6}\varepsilon$, there exists a function $\varphi_{z;T} \in C(\bar{T})$ such that*

$$\varphi_{z;T} = \phi_z \ \text{ on } \partial T, \qquad \|\varepsilon \operatorname{div}(\varphi_{z;T}\,\boldsymbol{\mu}_T)\|_T^2 \leqslant \|\varphi_{z;T}\|_T^2 = \tfrac{2}{\sqrt{6}}\varepsilon|T||S_T|^{-1} \lesssim \varepsilon H_T. \quad (7.2)$$

Proof. Introduce the two triangles $T^-, T^+ \subset T$, each $T^\pm$ formed by the edge $S_T^\pm$ and a common vertex lying on the median of T originating at z, subject to $|T^\pm| = \sqrt{6}\varepsilon|T||S_T|^{-1} < \frac{1}{4}|T|$ (see Fig. 7.2). Now, define a unique $\varphi_{z;T} \in C(\bar{T})$ that (i) satisfies $\varphi_{z;T} = \phi_z$ on ∂T; (ii) has support in $T^- \cup T^+$; (ii) is linear in each $T^\pm$. Clearly, $\|\varphi_{z;T}\|_T^2 = \frac{1}{6}(|T^-| + |T^+|)$. Furthermore, a calculation shows that $|\operatorname{div}(\varphi_{z;T}\,\boldsymbol{\mu}_T)| = |\partial_{\boldsymbol{\mu}_T}\varphi_{z;T}| \leqslant |S_T|^{-1}|T|/|T^\pm|$ so $|\varepsilon \operatorname{div}(\varphi_z \boldsymbol{\mu}_T)| \leqslant \frac{1}{\sqrt{6}}$ in $T^- \cup T^+$. Combining these observations, one gets (7.2) (with the final relation in (7.2) easily following from $|T| \simeq h_T H_T \lesssim |S_T| H_T$). ∎

7.1. Definition of $\boldsymbol{\tau}_z$ for $h_z \gtrsim \varepsilon$. Introduce a subset ω_z^* of ω_z and, using $\varphi_{z;T}$ from Lemma 7.3, a related function ϕ_z^*:

$$\omega_z^* := \Big\{T \subset \omega_z : |S_T| \simeq h_T \ll H_T\Big\}, \quad \phi_z^* := \begin{cases} \varphi_{z;T} & \text{on } \ T \subset \omega_z^* : |S_T| > 4\sqrt{6}\varepsilon, \\ \phi_z & \text{otherwise.} \end{cases} \quad (7.3)$$

Thus, ω_z^* includes only triangles with extremely small angles at z, so $\omega_z \backslash \omega_z^* \neq \varnothing$ (see Fig. 7.3). Note also that $\phi_z^* = \phi_z$ on γ_z. Now, using $\boldsymbol{\tau}_{z;T}^\pm$ from Lemma 7.1, set

$$\boldsymbol{\tau}_z := \begin{cases} \frac{1}{2}\Big(\mathcal{J}_z\big|_{S_T^-}\boldsymbol{\tau}_{z;T}^- + \mathcal{J}_z\big|_{S_T^+}\boldsymbol{\tau}_{z;T}^+\Big) & \text{for } \ T \subset \omega_z \backslash \omega_z^*, \\ (\beta_T d_T^{-1})\,\phi_z^*\,\boldsymbol{\mu}_T, \quad d_T := 2|T|\,|S_T|^{-1} & \text{for } \ T \subset \omega_z^*, \end{cases} \quad (7.4)$$

where, with the convention $[\partial_{\boldsymbol{\nu}} u_h]_{\partial\Omega} := 0$,

$$\mathcal{J}_z\big|_{S_T^\pm} := \begin{cases} \big[\partial_{\boldsymbol{\nu}} u_h\big]_{S_T^\pm} & \text{if } \ S_T^\pm \notin \partial\omega_z^*, \\ |S_T^\pm|^{-1} \displaystyle\sum_{S \in \gamma_{z;T}^\pm} |S| \big[\partial_{\boldsymbol{\nu}} u_h\big]_S & \text{otherwise.} \end{cases} \quad (7.5)$$

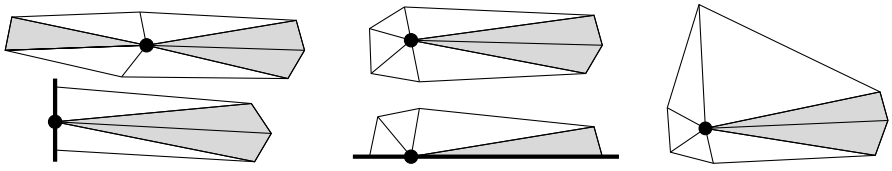

FIG. 7.3. *For various nodes, the set ω_z^* (defined in (7.3)) is highlighted by the grey color.*

To define $\gamma^{\pm}_{z;T}$ in (7.5), it is convenient to assume that ω^*_z includes triangles with their boundaries. Now, let $\omega^{\pm}_{z;T}$ be the maximal connected subset of $\omega^*_z\backslash\{z\}$ that shares the edge $S^{\pm}_T$ with T. The set of all edges originating at z that are contained in this subset $\omega^{\pm}_{z;T}$ (including $S^{\pm}_T$) is denoted $\gamma^{\pm}_{z;T}$.

The unique set of values $\{\beta_T\}$ for $T \subset \omega^*_z$ in (7.4) is chosen to satisfy (4.4). For example, consider a bundle of m triangles $\omega^+_{z;T} = \omega^-_{z;T'} = \{T_i\}_{i=1}^m$, numbered counterclockwise, that touches $T, T' \subset \omega_z\backslash\omega^*_z$. Now, (4.4) is equivalent to a version of (5.1c):

$$\beta_{i-1} - \beta_i = |S_i^-|[\partial_{\boldsymbol{\nu}} u_h]_{\partial T_{i-1}\cap\partial T_i}, \quad i = 1, \dots, m+1, \tag{7.6a}$$

where the notation $\beta_i := \beta_{T_i}$ is used for $i = 1, \dots, m$, while

$$\beta_0 = -\beta_{m+1} := \tfrac{1}{2}\sum_{i=1}^{m+1} |S_i^-|[\partial_{\boldsymbol{\nu}} u_h]_{\partial T_{i-1}\cap\partial T_i} = \tfrac{1}{2}|S_T^+|\,\mathcal{J}_z\big|_{S_T^+} = \tfrac{1}{2}|S_{T'}^-|\,\mathcal{J}_z\big|_{S_{T'}^-}. \tag{7.6b}$$

Note that the above system involves $m+1$ equations for $\{\beta_i\}_{i=1}^m$, but is consistent and has a unique solution. This becomes clear on application of $\sum_{i=1}^{m+1}$ to (7.6a) which yields a relation for $\beta_0 - \beta_{m+1}$ consistent with (7.6b).

If for a bundle of m triangles $\cup_{i=1}^m T_i = \omega^+_{z;T}$, numbered counterclockwise, one has $S_m^+ \subset \partial\Omega$, then we use (7.6a) with $i \neq m+1$, and β_0 from (7.6b) (while β_{m+1} remains undefined). Similarly, if $S_1^- \subset \partial\Omega$, then use (7.6a) with $i \neq 1$ combined with the definition of β_{m+1} from (7.6b) (and β_0 remaining undefined).

Remark 7.4 ($\gamma_z \cap \mathcal{S}^* \neq \varnothing$). Note that $\mathcal{S}^*$, defined by (6.1)*, can be chosen so that $\gamma_z \cap \mathcal{S}^* = \varnothing$ whenever $h_z \gtrsim \varepsilon$ under condition $\mathcal{A}2$ (as then $h_T \gtrsim \varepsilon$). If, however, $\gamma_z \cap \mathcal{S}^* \neq \varnothing$, then the non-trivial jumps $[\boldsymbol{\tau}_S^J \cdot \boldsymbol{\nu}]$ across γ_z are easily taken into account by replacing $[\partial_{\boldsymbol{\nu}} u_h]_{\partial T_{i-1}\cap\partial T_i}$ with $[\partial_{\boldsymbol{\nu}} u_h]_{\partial T_{i-1}\cap\partial T_i} + |S_i^-|^{-1}(\kappa_{i-1} - \kappa_{i+1})$ in* (7.5) *and* (7.6) *(where κ_i is defined in* (6.4)*). With this modification, Lemma 7.5 below remains valid as $|\kappa_i| \lesssim H_z|J_z|$ $\forall i$ (the latter follows from* (6.2)*).*

7.2. Proof of (4.8) **in Theorem 4.3 for** $h_z \gtrsim \varepsilon$**.** It suffices to prove the following.

LEMMA 7.5. *Under condition $\mathcal{A}2$, for any $z \in \mathcal{N}$ with $h_z \gtrsim \varepsilon$, the function $\boldsymbol{\tau}_z$ defined by* (7.1), (7.2), (7.3) (7.4), (7.5), (7.6) *satisfies* (4.4) *and*

$$\|\varepsilon^2 \operatorname{div}\boldsymbol{\tau}_z\|^2_{\omega_z} + \|\varepsilon\boldsymbol{\tau}_z\|^2_{\omega_z} \lesssim \sum_{S\in\gamma_z} \varepsilon|S| \left(\varepsilon[\partial_{\boldsymbol{\nu}} u_h]_S\right)^2 \lesssim \varepsilon h_z^{-1} \|\varepsilon J_z\|^2_{\omega_z}, \tag{7.7}$$

where $\varepsilon|S| \simeq \min\{\varepsilon|S|, |\omega_z|\}$ for any $S \in \gamma_z$.

Proof. Condition (4.4) is satisfied by the construction of $\boldsymbol{\tau}_z$ in §7.1, so it remains to establish (7.7).

First, for each fixed $S \in \gamma_z \cap \mathring{\mathcal{S}}_z$ (i.e. $|S| \simeq \mathring{h}_z$), we shall trace the contribution of $[\partial_{\boldsymbol{\nu}} u_h]_S$ to $\boldsymbol{\tau}_z$ of (7.4). In this case, $[\partial_{\boldsymbol{\nu}} u_h]_S$ is involved in $\boldsymbol{\tau}_z$ only on the triangles adjacent to S (such triangles are not in ω^*_z) in the form of the terms $\mathcal{J}_z\big|_S = [\partial_{\boldsymbol{\nu}} u_h]_S$. Hence, the contribution of the considered $[\partial_{\boldsymbol{\nu}} u_h]_S$ to the left-hand side of (7.7) is indeed bounded by $\varepsilon|S|(\varepsilon[\partial_{\boldsymbol{\nu}} u_h]_S)^2$, as can be shown by an application of (7.1b) with $|S_T^{\pm}| = |S|$ and $\varsigma^{-1}_{z;T} \simeq 1$. Furthermore, $|S| \lesssim H_z$ implies $\varepsilon|S| \lesssim \varepsilon h_z^{-1}|\omega_z|$ and so $\varepsilon|S|(\varepsilon[\partial_{\boldsymbol{\nu}} u_h]_S)^2 \lesssim \varepsilon h_z^{-1}\|\varepsilon[\partial_{\boldsymbol{\nu}} u_h]_S\|^2_{\omega_z}$.

It remains to bound the contribution to the left-hand side of (7.7) of $[\partial_{\boldsymbol{\nu}} u_h]_S$ for the edges $S \notin \mathring{\mathcal{S}}_z$. In this case, $|S| \simeq H_z$, so $\varepsilon|S|\big(\varepsilon[\partial_{\boldsymbol{\nu}} u_h]_S\big)^2 \simeq \varepsilon h_z^{-1}\big\|\varepsilon[\partial_{\boldsymbol{\nu}} u_h]_S\big\|^2_{\omega_z}$.

This observation implies that it now suffices to prove only the second relation in (7.7), or, equivalently, show that $\|\varepsilon\,\mathrm{div}\boldsymbol{\tau}_z\|_T^2 + \|\boldsymbol{\tau}_z\|_T^2 \lesssim \varepsilon H_z|J_z|^2$ for any $T \subset \omega_z$, to which we proceed.

Suppose $T \subset \omega_z^*$. By (7.3), $d_T \simeq H_T \simeq H_z$, and, by (7.6), $|\beta_T| \lesssim H_z|J_z|$, so $|d_T^{-1}\beta_T| \lesssim |J_z|$. Now, if $\phi_z^* = \varphi_{z;T}$ in T, then the desired bound on $\|\varepsilon\,\mathrm{div}\boldsymbol{\tau}_z\|_T^2 + \|\boldsymbol{\tau}_z\|_T^2$ follows from (7.2) combined with $\varepsilon H_T \leqslant \varepsilon H_z$. Otherwise, $\phi_z^* = \phi_z$ in T implies $\mathrm{div}\boldsymbol{\tau}_z = 0$ (see the proof of Lemma 5.1), and also $h_T \lesssim \varepsilon$ (in view of the definition of ϕ_z^* in (7.3)), so again $\|\boldsymbol{\tau}_z\|_T^2 \lesssim |T||J_z|^2 \lesssim \varepsilon H_z|J_z|^2$. Finally, suppose $T \subset \omega_z\backslash\omega_z^*$. Note that $|\mathcal{J}_z| \lesssim |J_z|$, which follows from (7.5) as $|S| \simeq |H_T|$ for all edges $S \in \gamma_{z;T}^{\pm}$ including $S_T^{\pm}$. Now, the desired bound on $\|\varepsilon\,\mathrm{div}\boldsymbol{\tau}_z\|_T^2 + \|\boldsymbol{\tau}_z\|_T^2$ follows from (7.1b) with $|S_T^{\pm}| \lesssim H_z$ and $\varsigma_{z;T}^{-1} \simeq 1$. □

8. Numerical results. Our estimator is tested using a simple version of (1.1) with $\Omega = (0,1)^2$ and $f = u - F(x,y)$, where F is such that the unique exact solution $u = 4y\,(1-y)\,[C_u\cos(\pi x/2) - (e^{-x/\varepsilon} - e^{-1/\varepsilon})/(1-e^{-x/\varepsilon})]$ (the latter exhibits a sharp boundary layer at $x = 0$); the constant parameter C_u in u will take values 1 and 0. We consider an a-priori-chosen layer-adapted non-obtuse triangulation, as on Fig. 8.1 (left), which is obtained by drawing diagonals from the tensor product of the Bakhvalov grid $\{\chi(\frac{i}{N})\}_{i=1}^N$ in the x-direction [5] and a uniform grid $\{\frac{j}{M}\}_{j=0}^M$ in the y-direction with $M = \frac{1}{2}N$. The continuous mesh-generating function $\chi(t) = t$ if $\varepsilon > \frac{1}{6}$; otherwise, $\chi(t) = 3\varepsilon\ln\frac{1}{1-2t}$ for $t \in (0, \frac{1}{2} - 3\varepsilon)$ and is linear elsewhere subject to $\chi(1) = 1$. Furthermore, to test our estimator on a mesh with obtuse triangles and, in particular, the role of the estimator components $\boldsymbol{\tau}_S^J$ in (4.3) for $S \in \mathcal{S}^*$, we distort the initial non-obtuse triangulation by moving some of the nodes upwards/downwards by $\min\{\mathring{h}_z,\ \frac{1}{8}H_z\}$; see Fig. 8.1 (right).

In our numerical experiments, we set $\mathcal{T}_0 := \varnothing$ in (3.3) and replace $\lesssim$ by $\leqslant$ in (3.3), (4.3), and when dealing with the two cases $h_z \lesssim \varepsilon$ and $h_z \not\lesssim \varepsilon$, as well as with $h_T \lesssim \varepsilon$ in (6.1). Also, we understand $a \ll b$ as $a \leqslant \frac{1}{5}b$ for any two quantities a and b (so, for example, (3.3) becomes $\mathcal{T}^* := \{T \in \mathcal{T} : h_T \leqslant \frac{1}{5}H_T \text{ and } h_T \leqslant \varepsilon\}$).

We compute the estimator $\mathcal{E}$ from (4.2) with $C_f := 1$ and $\boldsymbol{\tau}$ from (4.3), (4.6). For the non-obtuse mesh of Fig. 8.1 (left), conditions $\mathcal{A}1$ and $\mathcal{A}2$ are satisfied, so we set $\mathcal{S}^* = \varnothing$. The component $\boldsymbol{\tau}_z$ in (4.3) is computed by (5.1) combined with (5.3) for $h_z \leqslant \varepsilon$, and, otherwise, using (7.3), (7.4), (7.5) combined with (7.6). Note that instead of explicitly including the components involving $\boldsymbol{\tau}_{z;T}^{\pm}$ (from (7.4)) in $\boldsymbol{\tau}$, we use (7.1b) (as well as Remark 7.2). This somewhat simplifies the computations, but yields a slightly less sharp estimator. When computing the error and the estimator, we replace ∇u by its linear Lagrange interpolant, and u and f_h by their quadratic Lagrange interpolants.

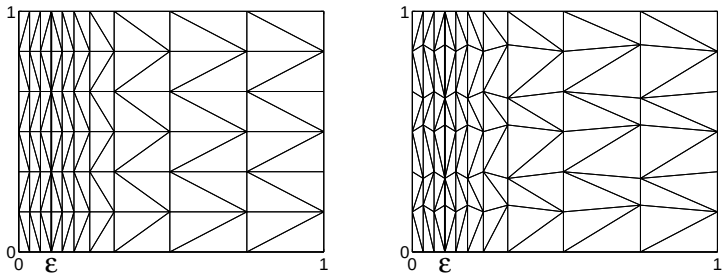

FIG. 8.1. *Non-obtuse triangulation used in §8 (left); its version with obtuse triangles (right).*

TABLE 8.1
Test problem with $C_u = 1$, non-obtuse triangulation (see Fig. 8.1, left), $\mathcal{S}^* = \varnothing$ in (4.3).

N	$\varepsilon = 1$	$\varepsilon = 2^{-5}$	$\varepsilon = 2^{-10}$	$\varepsilon = 2^{-15}$	$\varepsilon = 2^{-20}$	$\varepsilon = 2^{-25}$	$\varepsilon = 2^{-30}$
	Errors $\|\|\|u_h - u\|\|\|_{\varepsilon;\Omega}$						
64	3.203e-2	5.204e-3	1.065e-3	6.734e-4	6.576e-4	6.571e-4	6.571e-4
128	1.602e-2	2.594e-3	4.534e-4	1.797e-4	1.641e-4	1.636e-4	1.636e-4
256	8.011e-3	1.296e-3	2.157e-4	5.533e-5	4.133e-5	4.081e-5	4.080e-5
512	4.006e-3	6.479e-4	1.062e-4	2.130e-5	1.071e-5	1.020e-5	1.019e-5
	Estimators (odd rows) & Effectivity Indices (even rows)						
64	3.301e-2	6.959e-3	1.324e-3	6.878e-4	6.581e-4	6.572e-4	6.571e-4
	1.031	1.337	1.243	1.021	1.001	1.000	1.000
128	1.647e-2	2.698e-3	5.993e-4	1.928e-4	1.645e-4	1.636e-4	1.636e-4
	1.028	1.040	1.322	1.073	1.003	1.000	1.000
256	8.232e-3	1.335e-3	2.914e-4	6.541e-5	4.178e-5	4.083e-5	4.080e-5
	1.028	1.030	1.351	1.182	1.011	1.000	1.000
512	4.115e-3	6.668e-4	1.446e-4	2.753e-5	1.115e-5	1.022e-5	1.019e-5
	1.027	1.029	1.361	1.292	1.041	1.001	1.000

TABLE 8.2
Test problem with $C_u = 1$, mesh with obtuse triangles (see Fig. 8.1, right), $\mathcal{S}^* \neq \varnothing$ in (4.3).

N	$\varepsilon = 1$	$\varepsilon = 2^{-5}$	$\varepsilon = 2^{-10}$	$\varepsilon = 2^{-15}$	$\varepsilon = 2^{-20}$	$\varepsilon = 2^{-25}$	$\varepsilon = 2^{-30}$
	Errors $\|\|\|u_h - u\|\|\|_{\varepsilon;\Omega}$						
64	3.334e-2	5.311e-3	1.095e-3	7.218e-4	7.072e-4	7.067e-4	7.067e-4
128	1.669e-2	2.647e-3	4.580e-4	1.913e-4	1.768e-4	1.763e-4	1.763e-4
256	8.352e-3	1.323e-3	2.161e-4	5.774e-5	4.451e-5	4.404e-5	4.402e-5
512	4.177e-3	6.612e-4	1.061e-4	2.170e-5	1.149e-5	1.101e-5	1.100e-5
	Estimators (odd rows) & Effectivity Indices (even rows)						
64	3.546e-2	8.121e-3	1.534e-3	7.466e-4	7.080e-4	7.068e-4	7.067e-4
	1.064	1.529	1.401	1.034	1.001	1.000	1.000
128	1.772e-2	3.553e-3	7.077e-4	2.140e-4	1.776e-4	1.763e-4	1.763e-4
	1.062	1.342	1.545	1.118	1.005	1.000	1.000
256	8.866e-3	1.770e-3	3.461e-4	7.509e-5	4.532e-5	4.406e-5	4.402e-5
	1.061	1.338	1.601	1.300	1.018	1.001	1.000
512	4.434e-3	8.839e-4	1.719e-4	3.238e-5	1.225e-5	1.104e-5	1.100e-5
	1.062	1.337	1.621	1.492	1.066	1.002	1.000

When using the mesh with obtuse triangles of Fig. 8.1 (right), we consider $\mathcal{S}^*$ defined by (6.1), and also compare the latter with a simpler choice $\mathcal{S}^* = \varnothing$. Whenever $\mathcal{S}^* \neq \varnothing$, the estimator involves $\boldsymbol{\tau}_S^J$ computed by (6.2), while the computation of $\boldsymbol{\tau}_z$ employs (6.4) and Remark 7.4.

For the test problem with $C_u = 1$, the errors $\|\|\|u_h - u\|\|\|_{\varepsilon;\Omega}$ are compared with the corresponding estimators $\mathcal{E}$ in Tables 8.1 and 8.2. One observes that the effectivity indices (computed as the ratio of the estimator to the error) do not exceed 1.63. Note that for the same test problem, the estimator with $\mathcal{S}^* = \varnothing$ on the mesh with obtuse triangles exhibits larger and less stable effectivity indices. But the superiority of the estimator with $\mathcal{S}^* \neq \varnothing$ is particularly evident for the test problem with $C_u = 0$ on the mesh with obtuse triangles; compare the effectivity indices in Tables 8.3 and 8.4.

Overall, for the considered ranges of ε and N, the aspect ratios of the mesh elements take values between 2 and 3.6e+8. Considering these variations, our estimator $\mathcal{E}$ performs quite well and its effectivity indices do not exceed 1.63 and stabilize as

TABLE 8.3
Test problem with $C_u = 0$, mesh with obtuse triangles (see Fig. 8.1, right), $\mathcal{S}^* = \varnothing$ in (4.3).

N	$\varepsilon = 1$	$\varepsilon = 2^{-5}$	$\varepsilon = 2^{-10}$	$\varepsilon = 2^{-15}$	$\varepsilon = 2^{-20}$	$\varepsilon = 2^{-25}$	$\varepsilon = 2^{-30}$
	Errors $\|\|\|u_h - u\|\|\|_{\varepsilon;\Omega}$						
64	5.329e-2	4.862e-3	8.425e-4	1.489e-4	2.633e-5	4.655e-6	8.228e-7
128	2.680e-2	2.438e-3	4.222e-4	7.469e-5	1.320e-5	2.334e-6	4.126e-7
256	1.344e-2	1.220e-3	2.110e-4	3.740e-5	6.611e-6	1.169e-6	2.066e-7
512	6.727e-3	6.104e-4	1.051e-4	1.871e-5	3.308e-6	5.848e-7	1.034e-7
	Estimators (odd rows) & Effectivity Indices (even rows)						
64	5.729e-2	7.781e-3	1.487e-3	2.631e-4	4.652e-5	8.223e-6	1.454e-6
	1.075	1.600	1.765	1.767	1.767	1.767	1.767
128	2.881e-2	3.383e-3	8.710e-4	1.565e-4	2.766e-5	4.890e-6	8.645e-7
	1.075	1.388	2.063	2.095	2.095	2.095	2.095
256	1.444e-2	1.689e-3	5.883e-4	1.167e-4	2.063e-5	3.648e-6	6.448e-7
	1.075	1.384	2.788	3.121	3.121	3.121	3.121
512	7.231e-3	8.443e-4	3.903e-4	1.055e-4	1.866e-5	3.299e-6	5.832e-7
	1.075	1.383	3.713	5.638	5.642	5.642	5.642

TABLE 8.4
Test problem with $C_u = 0$, mesh with obtuse triangles (see Fig. 8.1, right), $\mathcal{S}^* \neq \varnothing$ in (4.3).

N	$\varepsilon = 1$	$\varepsilon = 2^{-5}$	$\varepsilon = 2^{-10}$	$\varepsilon = 2^{-15}$	$\varepsilon = 2^{-20}$	$\varepsilon = 2^{-25}$	$\varepsilon = 2^{-30}$
	Errors $\|\|\|u_h - u\|\|\|_{\varepsilon;\Omega}$						
64	5.329e-2	4.862e-3	8.425e-4	1.489e-4	2.633e-5	4.655e-6	8.228e-7
128	2.680e-2	2.438e-3	4.222e-4	7.469e-5	1.320e-5	2.334e-6	4.126e-7
256	1.344e-2	1.220e-3	2.110e-4	3.740e-5	6.611e-6	1.169e-6	2.066e-7
512	6.727e-3	6.104e-4	1.051e-4	1.871e-5	3.308e-6	5.848e-7	1.034e-7
	Estimators (odd rows) & Effectivity Indices (even rows)						
64	5.729e-2	7.687e-3	1.370e-3	2.422e-4	4.281e-5	7.568e-6	1.338e-6
	1.075	1.581	1.626	1.626	1.626	1.626	1.626
128	2.881e-2	3.330e-3	6.870e-4	1.215e-4	2.148e-5	3.797e-6	6.712e-7
	1.075	1.366	1.627	1.627	1.627	1.627	1.627
256	1.444e-2	1.660e-3	3.437e-4	6.086e-5	1.076e-5	1.902e-6	3.362e-7
	1.075	1.360	1.629	1.627	1.627	1.627	1.627
512	7.231e-3	8.301e-4	1.715e-4	3.046e-5	5.385e-6	9.519e-7	1.683e-7
	1.075	1.360	1.632	1.628	1.628	1.628	1.628

$\varepsilon \to 0$ and N increases (as long as $\mathcal{S}^* \neq \varnothing$ is used for the mesh with obtuse triangles). We have also observed that the inclusion of the estimator components $\boldsymbol{\tau}_S^J$ in (4.3) for $S \in \mathcal{S}^* \neq \varnothing$, in general, yields a superior estimator. A more comprehensive numerical study of the proposed estimator certainly needs to be conducted, and will be presented elsewhere.

9. Lower error bounds. Estimator efficiency. Throughout this section, we additionally assume that $f(x,y;u) - f(x,y;v) \lesssim |u - v|$, and use the additional notation $J_S := [\partial_{\boldsymbol{\nu}} u_h]_S$ and $\omega_S := T \cup T'$ for any $S = \partial T \cap \partial T' \in \mathcal{S}$ (with the obvious modification $\omega_S := T$ for the case $S \subset \partial T \cap \partial\Omega$).

9.1. Standard lower error bounds are not sharp. Numerical example. Consider a simple test problem (1.1) with $\varepsilon = 1$, the unique exact solution $u = \sin(\pi a x)$ (for $a = 1, 3$), and $f = u - F(x,y)$ on $\Omega = (0,1)^2$. We employ the triangulation obtained by drawing diagonals from the tensor product of the uniform

TABLE 9.1
Lower error estimators for test problem with $u = \sin(\pi a x)$ and $\varepsilon = 1$.

	$a = 1$			$a = 3$		
	$N = 20$	$N = 40$	$N = 80$	$N = 20$	$N = 40$	$N = 80$
	Errors $\|\|\|u_h - u\|\|\|_{\varepsilon;\Omega}$ (odd rows) & $\|h_T(f_h - f_h^I)\|_\Omega$ (even rows)					
$M = 2N$	1.01e-1	5.04e-2	2.52e-2	9.26e-1	4.56e-1	2.27e-1
	3.87e-4	4.84e-5	6.05e-6	2.87e-2	3.59e-3	4.50e-4
$M = 8N$	1.01e-1	5.04e-2	2.52e-2	9.26e-1	4.56e-1	2.27e-1
	1.07e-4	1.34e-5	1.68e-6	7.95e-3	9.97e-4	1.25e-4
$M = 32N$	1.01e-1	5.04e-2	2.52e-2	9.26e-1	4.56e-1	2.27e-1
	2.70e-5	3.38e-6	4.22e-7	2.00e-3	2.51e-4	3.14e-5
$M = 128N$	1.01e-1	5.04e-2	2.52e-2	9.26e-1	4.56e-1	2.27e-1
	6.76e-6	8.45e-7	1.06e-7	5.01e-4	6.28e-5	7.86e-6
	$\underline{\mathcal{E}}$ using $\varrho_{S([19])}$ (odd rows) & Effectivity Indices (even rows)					
$M = 2N$	2.89e-1	1.45e-1	7.24e-2	2.51e+0	1.26e+0	6.33e-1
	2.87	2.88	2.88	2.72	2.78	2.79
$M = 8N$	1.32e-1	6.59e-2	3.30e-2	1.17e+0	5.86e-1	2.93e-1
	1.31	1.31	1.31	1.26	1.29	1.29
$M = 32N$	6.27e-2	3.14e-2	1.57e-2	5.62e-1	2.82e-1	1.41e-1
	0.62	0.62	0.62	0.61	0.62	0.62
$M = 128N$	3.10e-2	1.55e-2	7.75e-3	2.79e-1	1.39e-1	6.97e-2
	0.31	0.31	0.31	0.30	0.31	0.31
	$\underline{\mathcal{E}}$ using $\varrho_{S(\S9.3)}$ (odd rows) & Effectivity Indices (even rows)					
$M = 2N$	3.00e-1	1.50e-1	7.52e-2	2.61e+0	1.32e+0	6.59e-1
	2.98	2.98	2.98	2.82	2.89	2.90
$M = 8N$	2.51e-1	1.26e-1	6.28e-2	2.25e+0	1.13e+0	5.64e-1
	2.49	2.49	2.49	2.43	2.47	2.48
$M = 32N$	2.47e-1	1.23e-1	6.18e-2	2.21e+0	1.11e+0	5.56e-1
	2.45	2.45	2.45	2.39	2.44	2.45
$M = 128N$	2.46e-1	1.23e-1	6.17e-2	2.21e+0	1.11e+0	5.55e-1
	2.44	2.45	2.45	2.39	2.43	2.45

grids $\{\frac{i}{N}\}_{i=0}^N$ and $\{\frac{j}{M}\}_{j=0}^M$ respectively in the x- and y-directions (with all diagonals having the same orientation). The standard lumped-mass quadrature, i.e. $\mathcal{T}_* := \varnothing$ in (3.2), will be used in numerical experiments in this section (while the anisotropic quadrature with $\mathcal{T}_* := \mathcal{T}$ produces very similar results on this mesh).

For this problem, we compare two lower error estimators: obtained using the standard bubble function approach [19] (see also Lemma 9.1 in §9.2) and the one obtained in §9.3 (combine Theorem 9.4 with Lemma 9.1). They can be described by

$$\underline{\mathcal{E}} := \Big\{ \sum_{S\in\mathcal{S}\backslash\partial\Omega} \varrho_S\, J_S^2 + \|h_T f_h^I\|_\Omega^2 \Big\}^{1/2} \lesssim |\!|\!| u_h - u |\!|\!|_{\varepsilon;\Omega} + \|h_T(f_h - f_h^I)\|_\Omega, \tag{9.1a}$$

where the weight ϱ_S for $S \in \mathcal{S}\backslash\partial\Omega$ is defined by

$$\varrho_S = \begin{cases} \varrho_{S([19])} = |S| \min\limits_{T\subset\omega_S}\{h_T\}, & \text{[19] using bubble functions (also §9.2),} \\ \varrho_{S(\S9.3)} = \frac{1}{2}|\omega_S|, & \text{see Theorem 9.4 in §9.3.} \end{cases} \tag{9.1b}$$

(To be more precise, when $\varrho_{S(\S9.3)}$ is used, the term $\|h_T(f_h - f_h^I)\|_\Omega$ in the right-hand

side of (9.1a) should be replaced by a larger $\|\lambda_T \operatorname{osc}(f_h\,;T)\|_\Omega$; see §9.3 for details.)

To address whether the left-hand side $\underline{\mathcal{E}}$ in (9.1a) is sharp, the errors $\|\!|\!| u_h - u |\!|\!|_{\varepsilon\,;\Omega}$ (as well as $\|h_T(f_h - f_h^I)\|_\Omega$) are compared with $\underline{\mathcal{E}}$ in Table 9.1. Clearly, the standard lower estimator using the weights $\varrho_{S([19])}$ is not sharp. Not only its effectivity indices strongly depend on the ratio M/N, but, perhaps more alarmingly, $\underline{\mathcal{E}}$ converges to zero as M/N increases, i.e. the mesh is anisotropically refined in the wrong direction (while the error remains almost independent of M/N). By contrast, the estimator of §9.3 performs quite well, with the effectivity indices stabilizing.

When comparing the two estimators, note that $\varrho_{S([19])} \simeq \varrho_{S(\S 9.3)}$ when $|S| \simeq \operatorname{diam}\omega_S$, however, $\varrho_{S([19])} \ll \varrho_{S(\S 9.3)}$ when $|S| \ll \operatorname{diam}\omega_S$, i.e. for short edges. Hence, our numerical experiments suggest that it is the short-edge jump residual terms in the standard lower estimator that are not sharp. We shall address this theoretically in §9.3.

9.2. Lower error bounds using the standard bubble approach. Here, for completeness, we prove a version of the lower error bounds from [19, Theorem 4.3] for the semilinear case (similar, but less sharp bounds can also be found in [18, 20]).

LEMMA 9.1. *For a solution u of (1.1) and any $u_h \in S_h$, one has*

$$\min\{1,\, h_T\varepsilon^{-1}\}\|f_h^I\|_T \lesssim \underbrace{\|\!|\!| u_h - u |\!|\!|_{\varepsilon\,;T} + \min\{1,\, h_T\varepsilon^{-1}\}\|f_h - f_h^I\|_T}_{=:\mathcal{Y}_T} \quad \forall T \in \mathcal{T}, \tag{9.2a}$$

$$|S|^{1/2}\,\big|\varepsilon J_S\big| \lesssim \sum_{T\in\omega_S} \mathcal{Y}_T\, \min\{\varepsilon,\, h_T\}^{-1/2} \qquad \forall S \in \mathcal{S}\backslash\partial\Omega. \tag{9.2b}$$

COROLLARY 9.2. *If $|\omega_z| \simeq |T|$ for any $T \subset \omega_z$, then*

$$\min\{1,\, \varepsilon h_z^{-1}\}^{1/2}\, \|\varepsilon\widetilde{J}_z\|_{\omega_z} + \min\{1,\, h_z\varepsilon^{-1}\}\|f_h^I\|_{\omega_z} \lesssim \sum_{T\subset\omega_z} \mathcal{Y}_T\,,$$

where

$$\widetilde{J}_z := \underbrace{\max_{S\in\gamma_z:|S|\simeq H_z} \big|J_S\big|}_{=:\widehat{J}_z} + \{h_z H_z^{-1}\}^{1/2} \underbrace{\max_{S\in\gamma_z:|S|\ll H_z} \big|J_S\big|}_{=:\mathring{J}_z}.$$

*Remark 9.3 (*Estimator efficiency under an adaptive-mesh-alignment condition*). It appears that the above result is as sharp as one can get using the bubble function approach, while in §9.1 we have seen that the short-edge jump residual terms are not sharp in such bounds. On the other hand, the interpolation error bounds suggest that a reasonably optimal and correctly-aligned mesh may be expected to satisfy $\mathring{J}_z \lesssim \widehat{J}_z$. Consequently, it appears reasonable to impose a mild version of this condition:*

$$\varepsilon\mathring{J}_z \lesssim \varepsilon\widehat{J}_z + \min\{1,\, \varepsilon h_z^{-1}\}^{-1/2} \min\{1,\, h_z\varepsilon^{-1}\}\|f_h^I\|_{L_\infty(\omega_z)}. \tag{9.3}$$

when constructing a mesh adaptively. Clearly, if both (9.3) and the condition of the above corollary are satisfied for all $z \in \mathcal{N}$, then the upper error estimator from (1.2) is efficient.

Proof of Lemma 9.1. (i) On any $T \in \mathcal{T}$, consider $w := f_h^I\,\phi_1\phi_2\phi_3$, where $\{\phi_i\}_{i=1}^3$ are the standard hat functions associated with the three vertices of T. Now, a standard calculation yields $\|f_h^I\|_T^2 \simeq \langle f_h^I, w\rangle$. So, using $f_h^I = -\varepsilon^2\triangle u_h + f_h^I$ and (1.1) yields $\|f_h^I\|_T^2 \simeq \varepsilon^2\langle\nabla(u_h - u), \nabla w\rangle + \langle f_h^I - f(\cdot\,;u), w\rangle$. Next, invoking $\|\nabla w\|_T \lesssim h_T^{-1}\|w\|_T$, one arrives at

$$\|f_h^I\|_T^2 \lesssim \Big((\varepsilon h_T^{-1} + 1)\|\!|\!| u_h - u |\!|\!|_{\varepsilon\,;T} + \|f_h - f_h^I\|_T\Big)\,\|w\|_T\,.$$

Here we also used $|f_h^I - f(\cdot;u)| \lesssim |u_h - u| + |f_h - f_h^I|$. The desired result (9.2a) follows in view of $\|w\|_T \lesssim \|f_h^I\|_T$ and $\varepsilon h_T^{-1} + 1 \simeq \min\{1,\, h_T\varepsilon^{-1}\}^{-1}$.

(ii) For each of the two triangles $T \subset \omega_S$, introduce a triangle $\widetilde{T} \subseteq T$ with an edge S such that $|\widetilde{T}| \simeq \min\{\varepsilon,\, h_T\}|S|$. Next, set $w := J_S\,\widetilde{\phi}'\widetilde{\phi}''$, where $\widetilde{\phi}'$ and $\widetilde{\phi}''$ are the hat functions on the triangulation $\{\widetilde{T}\}_{T\subset\omega_S}$ associated with the two end points of S (with $w := 0$ on each $T\backslash\widetilde{T}$ for $T \subset \omega_S$). A standard calculation using $\triangle u_h = 0$ in $T \subset \omega_S$ and (1.1), yields

$$|S|\,(\varepsilon J_S)^2 \simeq \varepsilon^2 \int_S w\,[\partial_{\boldsymbol{\nu}} u_h]_S = \varepsilon^2\langle\nabla u_h, \nabla w\rangle = \varepsilon^2\langle\nabla(u_h - u), \nabla w\rangle - \langle f(\cdot;u), w\rangle.$$

Next, invoking $\|\nabla w\|_T \lesssim \min\{\varepsilon,\, h_T\}^{-1}\|w\|_T$ for any $T \subset \omega_S$, we arrive at

$$|S|\,(\varepsilon J_S)^2 \lesssim \sum_{T\in\omega_S} \underbrace{\Big(\min\{1,\, h_T\varepsilon^{-1}\}^{-1}|\!|\!|u_h - u|\!|\!|_{\varepsilon;T} + \|f_h\|_T\Big)}_{\lesssim \mathcal{Y}_T \min\{1,\, h_T\varepsilon^{-1}\}^{-1} \text{ by (9.2a)}} \underbrace{\|w\|_T}_{\simeq \min\{\varepsilon,\, h_T\}^{1/2}|S|^{1/2}|J_S|}.$$

In view of $\min\{1,\, h_T\varepsilon^{-1}\}^{-1}\,\min\{\varepsilon,\, h_T\}^{1/2}\,\varepsilon^{-1} \simeq \min\{\varepsilon,\, h_T\}^{-1/2}$, one gets (9.2b). ∎

9.3. New lower error bound with sharp short-edge jump residual terms. Throughout this section, we make additional restrictions on the anisotropic mesh as follows. Let $\Omega := (0,1)^2$, and $\{x_i\}_{i=0}^n$ be an arbitrary mesh in the x direction on the interval $(0,1)$. Then, let each $T \in \mathcal{T}$, for some i, (i) have the shortest edge on the line $x = x_i$; (ii) have a vertex on the line $x = x_{i+1}$ or $x = x_{i-1}$ (see Fig. 9.1). Also, let $\mathcal{N} = \mathcal{N}_{\rm ani}$, i.e. each $z \in \mathcal{N}$ be an anisotropic node in the sense of (2.3) and satisfy $\mathcal{A}1_{\rm ani}$. The above conditions essentially imply that all mesh elements are anisotropic and aligned in the x-direction. The main result of this section is the following.

THEOREM 9.4 (Short-edge jump residual terms). *Let u and u_h respectively satisfy* (1.1) *and* (3.1)*, and $\Omega_i := (x_{i-1}, x_{i+1}) \times (0,1)$. If either no no quadrature is used in Ω_i (i.e.* (3.1) *involves $\langle f_h, v_h\rangle_h = \langle f_h, v_h\rangle$ $\forall v_h \in S_h$ with support in Ω_i), or $\langle\cdot,\cdot\rangle_h$ is defined by* (3.2)–(3.5) *with either $\mathcal{T} \cap \Omega_i \subset \mathcal{T}^*$, or $\Omega_i \cap \mathcal{T}^* = \varnothing$, then*

$$\sum_{S\in\mathcal{S}\cap\{x=x_i\}} \min\{\varepsilon|S|, |\omega_S|\}\,\big(\varepsilon J_S\big)^2 \lesssim \underbrace{|\!|\!|u_h - u|\!|\!|_{\varepsilon;\Omega_i}^2 + \|\lambda_T\,\mathrm{osc}(f_h\,;T)\|_{\Omega_i}^2}_{=\sum_{T\subset\Omega_i}\mathcal{Y}_T^2\,=:\,\mathcal{Y}_i^2}. \tag{9.4}$$

To prove this theorem, we shall use an auxiliary result.

LEMMA 9.5. *(i) If $\gamma_z \cap \{x = x_i\}$ is formed by exactly two edges S^- and S^+, then*

$$\big|J_{S^+} - J_{S^-}\big| \lesssim h_z H_z^{-1} \sum_{S\in\gamma_z\backslash\{x=x_i\}} |J_S|. \tag{9.5}$$

(ii) If $\gamma_z \cap \{x = x_i\}$ is formed by a single edge S^+, then J_{S^-} in (9.5) *is replaced by* 0.

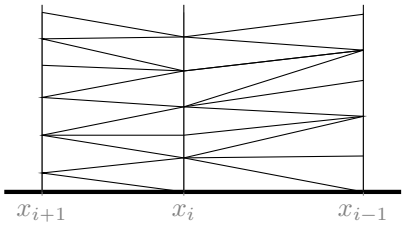

FIG. 9.1. *Partially structured anisotropic mesh considered in §9.3.*

Proof. (i) Note that in this case $z \notin \partial\Omega$. Using the notation $\{T_i\}$ of §5 (see Fig. 5.1, centre), let $[\![\nabla u_h]\!]_{\partial T_{i-1}\cap\partial T_i} := \nabla u_h\big|_{\partial T_i} - \nabla u_h\big|_{\partial T_{i-1}}$. Then $\sum_{S\in\gamma_z}[\![\nabla u_h]\!]_S = 0$. Multiplying this relation by the unit vector $\mathbf{i}_x$ in the x-direction, and noting that $[\![\nabla u_h]\!]_{S^\pm}\cdot\mathbf{i}_x = \pm J_{S^\pm}$, one gets the desired assertion. We also use the observation that for $S\in\gamma_z\backslash\{x=x_i\}$, one has $|[\![\nabla u_h]\!]_S\cdot\mathbf{i}_x| \simeq |J_S\,\boldsymbol{\nu}_S\cdot\mathbf{i}_x|$, where $\boldsymbol{\nu}_S$ is a unit vector normal to S, where, in view of $\mathcal{A}1_{\rm ani}$, one has $|\boldsymbol{\nu}_S\cdot\mathbf{i}_x| \lesssim h_z H_z^{-1}$.

(ii) Now $z\in\partial\Omega$, so extend u_h to $\mathbb{R}^2\backslash\Omega$ by 0 and imitate the above proof with the modification that now $\sum_{S\in\mathcal{S}_z}[\![\nabla u_h]\!]_S = 0$. When dealing with the two edges on $\partial\Omega$, note that for $S\in\mathcal{S}_z\cap\partial\Omega$, one gets $\boldsymbol{\nu}_S\cdot\mathbf{i}_x = 0$. □

Proof of Theorem 9.4. Set $H := x_{i+1}-x_{i-1}$, and $\theta := \min\{\varepsilon H^{-1}, \frac12\}$, and then $\widetilde{x}_{i\pm1} := x_i \pm \theta|x_{i\pm1}-x_i|$ and $\widetilde{\Omega}_i := (\widetilde{x}_{i-1},\widetilde{x}_{i+1})\times(0,1)$ (so Ω_i is a rectangular domain, at least, twice as narrow as Ω_i). Furthermore, define a triangulation $\widetilde{\mathcal{T}}_i$ on $\widetilde{\Omega}_i$ by dividing each trapezoid in the partition $\mathcal{T}\cap\widetilde{\Omega}_i$ into two triangles.

Now, define $v\in C(\bar\Omega)$ with support in $\widetilde{\Omega}_i$ (so $v=0$ on $\partial\widetilde{\Omega}_i$) using the standard piecewise-linear interpolation on $\widetilde{\mathcal{T}}_i$. Its node values in the interior of $\widetilde{\Omega}_i$ are defined by $v(z) := J_S$ for any $z\in\mathcal{N}$ on $\{x=x_i\}\backslash\partial\Omega$, where $S\in\gamma_z\cap\{x=x_i\}$ is any vertical short edge originating at z. (For definiteness, let S connect z with the node above it.)

Also, let $v_h\in S_h$ be the piecewise-linear interpolant of v on the original triangulation $\mathcal{T}$ (then $v\in C(\bar\Omega)$ has support in Ω_i), and $w := v-\theta v_h$. Now, a standard calculation yields

$$\begin{aligned}\underbrace{\varepsilon^2\langle\nabla(u_h-u),\nabla v\rangle + \langle\widehat{f}_h - f(\cdot;u), v\rangle}_{=:\psi_1} &= \varepsilon^2\langle\nabla u_h,\nabla v\rangle + \langle\widehat{f}_h, v\rangle\,,\\ &= \varepsilon^2\langle\partial_x u_h,\partial_x w\rangle + \underbrace{\varepsilon^2\langle\partial_y u_h,\partial_y w\rangle + \langle\widehat{f}_h, v\rangle - \theta\langle\widehat{f}_h, v_h\rangle_h}_{=:\psi_2}\,.\end{aligned} \tag{9.6}$$

Here we used a function $\widehat{f}_h \approx f_h$, which will be specified later subject to the condition $\|\lambda_T(\widehat{f}_h - f_h)\|_{\Omega_i} \lesssim \|\lambda_T\,\mathrm{osc}(f_h\,;T)\|_{\Omega_i} \leqslant \mathcal{Y}_i$.

With $\boldsymbol{\nu}_x := (\boldsymbol{\nu}\cdot\mathbf{i}_x)\mathbf{i}_x$ (which is the standard vector projection of the outward normal vector $\boldsymbol{\nu}$ onto $\mathbf{i}_x$), one gets

$$\langle\partial_x u_h,\partial_x w\rangle = \sum_{S\subset\mathcal{S}\cap\Omega_i}\int_S[\nabla u_h\cdot\boldsymbol{\nu}_x]w = \sum_{S\subset\mathcal{S}\cap\{x=x_i\}}\int_S[\nabla u_h\cdot\boldsymbol{\nu}_x]w,$$

where for $S\subset\mathcal{S}\cap\Omega_i\backslash\{x=x_i\}$, we used $\int_S w = \int_S v - \theta\int_S v_h = 0$ (as each of v and v_h is linear on its support on S, and $v=v_h$ on $\{x=x_i\}$). Next, note that for $S\subset\mathcal{S}\cap\{x=x_i\}$, one has $|S|\simeq H^{-1}|\omega_S|$, while $[\nabla u_h\cdot\boldsymbol{\nu}_x] = J_S$ and $w=(1-\theta)v$ with $v\geqslant J_S - \mathrm{osc}(v\,;S)$ (as $v=J_S$ at one of the end points of S), so

$$\langle\partial_x u_h,\partial_x w\rangle \geqslant (1-\theta)H^{-1}\sum_{S\subset\mathcal{S}\cap\{x=x_i\}}|\omega_S|\,J_S\big\{J_S - \mathrm{osc}(v\,;S)\big\}.$$

Combining the latter with (9.6) multiplied by θH, and noting that $1-\theta\geqslant\frac12$, one now gets

$$\sum_{S\subset\mathcal{S}\cap\{x=x_i\}}\theta|\omega_S|\,(\varepsilon J_S)^2 \lesssim \sum_{S\subset\mathcal{S}\cap\{x=x_i\}}\theta|\omega_S|\,\big(\varepsilon\,\mathrm{osc}(v\,;S)\big)^2 + (\theta H)|\psi_1-\psi_2|\,. \tag{9.7}$$

We claim that, to complete the proof, it suffices to get a somewhat similar bound:

$$\sum_{S\subset\mathcal{S}\cap\{x=x_i\}} \theta|\omega_S|\,(\varepsilon J_S)^2 \lesssim \mathcal{Y}_i^2 + \sum_{S\subset\mathcal{S}\cap\{x=x_i\}} \theta|\omega_S|\,\big(\varepsilon H|S|^{-1}\operatorname{osc}(v\,;S)\big)^2. \tag{9.8}$$

Indeed, this implies (9.4), as here in the left-hand side, $\theta|\omega_S| \simeq \min\{\varepsilon|S|, |\omega_S|\}$. Furthermore, using Lemma 9.5 to estimate $\operatorname{osc}(v\,;S)$, the sum in the right-hand side of (9.8) is bounded by $\sum_{S\subset\mathcal{S}\cap\Omega_i\setminus\{x=x_i\}} \theta|\omega_S|\,(\varepsilon J_S)^2 \lesssim \sum_{T\subset\Omega_i} \mathcal{Y}_T^2 \simeq \mathcal{Y}_i^2$. The latter assertion follows from (9.2b) in view of $\theta|\omega_S| \simeq \min\{\varepsilon h_T, |\omega_S|\} \lesssim \min\{\varepsilon|S|, h_T|S|\}$ for any $T\subset\omega_S$. So it remains to derive (9.8) from (9.7).

For ψ_1, defined in (9.6), in view of $|f_h - f(\cdot\,;u)| \lesssim |u_h - u|$ and $\|\lambda_T(\widehat{f}_h - f_h)\|_{\Omega_i} \lesssim \mathcal{Y}_i$, one has

$$|\psi_1| \lesssim \mathcal{Y}_i \Big\{\varepsilon\|\nabla v\|_{\widetilde{\Omega}_i} + \|\lambda_T^{-1} v\|_{\widetilde{\Omega}_i}\Big\}. \tag{9.9a}$$

Here, recalling the definition of v, note that $\partial_y v = 0$ in any triangle in $\widetilde{\mathcal{T}}_i$ with a single vertex on $\{x = x_i\}$, while $\partial_y v = \pm|S|^{-1}\operatorname{osc}(v\,;S)$ and $|\widetilde{T}| \simeq \theta|\omega_S|$ for any triangle $\widetilde{T}\in\widetilde{\mathcal{T}}_i$ sharing an edge S with $\{x = x_i\}$, so

$$\|\varepsilon\,\partial_y v\|_{\widetilde{\Omega}_i}^2 \lesssim \sum_{S\subset\mathcal{S}\cap\{x=x_i\}} \theta|\omega_S|\,\big(\varepsilon|S|^{-1}\operatorname{osc}(v\,;S)\big)^2. \tag{9.9b}$$

Furthermore, any triangle $\widetilde{T}\in\widetilde{\mathcal{T}}_i$ touches an edge $S\subset\{x = x_i\}$ such that $|\varepsilon\,\partial_x v| \lesssim \varepsilon(\theta H)^{-1}\max_{\widetilde{T}}|v| = \varepsilon(\theta H)^{-1} J_S$, while $\lambda_T^{-1} \simeq \varepsilon(\theta H)^{-1}$ implies a similar bound for $|\lambda_T^{-1} v|$. Combining these observations with $|\widetilde{T}| \simeq \theta|\omega_S|$ yields

$$\|\varepsilon\,\partial_x v\|_{\widetilde{\Omega}_i}^2 + \|\lambda_T^{-1} v\|_{\widetilde{\Omega}_i}^2 \lesssim \sum_{S\subset\mathcal{S}\cap\{x=x_i\}} \theta|\omega_S|\,\big(\varepsilon(\theta H)^{-1} J_S\big)^2 = (\theta H)^{-2} \sum_{S\subset\mathcal{S}\cap\{x=x_i\}} \theta|\omega_S|\,(\varepsilon J_S)^2. \tag{9.9c}$$

To estimate ψ_2 (defined in (9.6)), set $\widehat{f}_h(x,y) := f_h^I(x_i,y)$ and $\widehat{v}(x,y) := v(x_i,y)$ in Ω_i. Note that

$$\langle \partial_y u_h, \partial_y v\rangle = \theta\langle \partial_y u_h, \partial_y v_h\rangle, \qquad \int_{\widetilde{\Omega}_i} \widehat{f}_h\widehat{v}\,\widetilde{\varphi}_i(x) = \theta\int_{\Omega_i} \widehat{f}_h\widehat{v}\,\varphi_i(x), \tag{9.10}$$

where $\widetilde{\varphi}_i(x)$ and $\varphi_i(x)$ are the standard one-dimensional hat functions on the intervals $(\widetilde{x}_{i-1}, \widetilde{x}_{i+1})$ and (x_{i-1}, x_{i+1}), respectively, with $\widetilde{\varphi}_i(x_i) = \varphi_i(x_i) = 1$. For the first relation in (9.10), we relied on the observations made on $\partial_y v$ when obtaining (9.9b), as well as similar properties of v_h.

First, consider the case of no quadrature used in Ω_i, i.e. $\langle \widehat{f}_h, v\rangle_h = \langle \widehat{f}_h, v\rangle$. Then

$$\psi_2 = \int_{\widetilde{\Omega}_i} \widehat{f}_h\big(v - \widehat{v}\,\widetilde{\varphi}_i(x)\big) - \theta\int_{\Omega_i} \widehat{f}_h\big(v_h - \widehat{v}\,\varphi_i(x)\big). \tag{9.11}$$

From this one can show (we shall comment on this below) that

$$|\psi_2| \lesssim \underbrace{\big\|\min\{1,\, h_T\varepsilon^{-1}\}\,f_h^I\big\|_{\Omega_i}}_{\lesssim\mathcal{Y}_i \text{ by (9.2a)}} \Big\{\sum_{S\in\mathcal{S}\cap\{x=x_i\}} \theta|\omega_S|\,\big(\underbrace{\min\{1,\,|S|\varepsilon^{-1}\}^{-1}}_{\lesssim\varepsilon|S|^{-1}\theta^{-1}}\operatorname{osc}(v\,;S)\big)^2\Big\}^{1/2}. \tag{9.12}$$

Now, combining (9.9) and (9.12) with (9.7) one arrives at the desired assertion (9.8).

To complete the proof, we still need to show that that (9.12) follows from (9.11), as well as $\|\lambda_T(\widehat{f}_h - f_h)\|_{\Omega_i} \lesssim \|\lambda_T \operatorname{osc}(f_h\,;T)\|_{\Omega_i}$. For each $T \subset \Omega_i$, introduce the minimal rectangle $R_T = (x_{i-1}, x_{i+1}) \times (y_T^-, y_T^+)$ containing T (i.e. (y_T^-, y_T^+) is the range of y values within T). Note that, crucially, by condition $\mathcal{A}1_{\mathrm{ani}}$ there is $K \lesssim 1$ such that $|R_T| \simeq |T|$ and $R_T \subset \omega_T^{(K)} \cap \Omega_i$, with the notation $\omega_T^{(j+1)}$ for the patch of elements in/touching $\omega_T^{(j)}$ and $\omega_T^{(0)} := T$. Now, $|v - \widehat{v}\,\widetilde{\varphi}_i| \leqslant \operatorname{osc}(v\,; R_T \cap \{x = x_i\})$ for any $T \subset \Omega_i$, so (9.11) implies a version of (9.12) with f_h^I replaced by $\widehat{f}_h$, and $\operatorname{osc}(v\,;S)$ replaced by $\operatorname{osc}(v\,; R_T \cap \{x = x_i\})$. As $h_{T'} \simeq h_T$ and $H_{T'} \simeq H_T$ for any triangle $T' \cap R_T \neq \varnothing$, (9.12) follows. Similarly, $|\widehat{f}_h - f_h| \leqslant \operatorname{osc}(f_h^I\,; R_T)$ for any $T \subset \Omega_i$ implies $\|\lambda_T(\widehat{f}_h - f_h)\|_{\Omega_i} \lesssim \|\lambda_T \operatorname{osc}(f_h\,;T)\|_{\Omega_i}$.

Finally note that (9.11) is valid only if no quadrature is used in Ω_i. Otherwise, the estimation of ψ_2 needs to be slightly adjusted. For the case $\mathcal{T} \cap \Omega_i \subset \mathcal{T}^*$, tweak the definition of $\widehat{f}_h$ to $\widehat{f}_h(x,y) := \bar{f}_i(y)$, where $\bar{f}_i(y)$ is a one-dimensional piecewise-constant interpolant of f_h on $\{x = x_i\} \cap \Omega$ such that it is constant on each edge $S \subset \{x = x_i\}$. With this modification, $\int_{\Omega_i} \widehat{f}_h \widehat{v}\,\widetilde{\varphi}_i(x) = \langle \widehat{f}_h, v\rangle_h$, so the second term in (9.11) vanishes, while all other arguments apply. For the case $\Omega_i \cap \mathcal{T}^* = \varnothing$, one has $\langle \widehat{f}_h, v\rangle_h = \int_\Omega (\widehat{f}_h, v)^I$, so the bound (9.12) on ψ_2 will additionally include $\|\lambda_T \operatorname{osc}(f_h^I\,;T)\|_{\Omega_i} \|\lambda_T^{-1} v\|_{\widetilde{\Omega}_i}$, so (9.9c) is employed again for this additional term. ∎

Remark 9.6. Combing the lower error bounds (9.2) *and* (9.4) *and comparing the resulting lower bound with the upper error bound* (1.2)*, one concludes that for the estimator to be efficient, the term* $\min\{1, \varepsilon h_z^{-1}\}\|\varepsilon J_z\|_{\omega_z}^2$ *should be replaced by* $\sum_{S\in\gamma_z} \min\{\varepsilon|S|, |\omega_z|\}\,(\varepsilon J_S)^2$ *in* (1.2)*, and, equivalently, in* (4.8)*. When* $h_z \gtrsim \varepsilon$*, this improvement follows from the first relation in* (7.7)*. Otherwise, if* $H_z \lesssim \varepsilon$*, this follows from* $|\omega_z| \lesssim \varepsilon|S|$*. For the remaining case* $h_z \lesssim \varepsilon \lesssim H_z$*, assuming* $z \in \mathcal{N}_{\mathrm{ani}}$ *under condition* $\mathcal{A}1_{\mathrm{ani}}$*, this sharper upper bound can be shown for a slightly more intricate version of* $\boldsymbol{\tau}_z$*, defined as follows. Using the notation of* (5.1a) *and* (7.1) *(see Fig. 5.1 and Fig. 5.3 (left); also assume that* $\boldsymbol{\tau}_{z;T}^{\pm} \in L_2(\Omega)$ *has support on* T*), set*

$$\boldsymbol{\tau}_z := \sum_{i=1,m_z} \tfrac{1}{2} J_{S_i^-} \big(\boldsymbol{\tau}_{z;T_{i-1}}^{+} + \boldsymbol{\tau}_{z;T_i}^{-}\big) + \phi_z \sum_{i=1}^{N_z} \big(\alpha_i \boldsymbol{\nu}_i + \beta_i d_i^{-1} \boldsymbol{\mu}_i\big)\, \mathbb{1}_{(x,y)\in T_i}\,,$$

where $\{\alpha_i\}$ *and* $\{\beta_i\}$ *are chosen to minimize* (5.4) *subject to the constraints* (5.1c)*, in which* $\big[\partial_{\boldsymbol{\nu}} u_h\big]_{\partial T_{i-1}\cap\partial T_i}$ *for* $i = 1, m_z$ *are replaced by* 0*. It appears, however, that in most practical situations, this modification of* $\boldsymbol{\tau}_z$ *will not improve the estimator, as the short-edge jump residual terms in the upper error estimator are expected to be dominated by the other terms (as discussed in Remark 9.3).*

REFERENCES

[1] M. Ainsworth and I. Babuška, *Reliable and robust a posteriori error estimating for singularly perturbed reaction-diffusion problems*, SIAM J. Numer. Anal., 36 (1999), pp. 331–353.

[2] M. Ainsworth and J. T. Oden, *A posteriori error estimation in finite element analysis*, Wiley-Interscience, New York, 2000.

[3] M. Ainsworth and T. Vejchodský, *Fully computable robust a posteriori error bounds for singularly perturbed reaction-diffusion problems*, Numer. Math., 119 (2011), pp. 219–243.

[4] M. Ainsworth and T. Vejchodský, *Robust error bounds for finite element approximation of reaction-diffusion problems with non-constant reaction coefficient in arbitrary space dimension*, Comput. Methods Appl. Mech. Engrg., 281 (2014), pp. 184–199.

[5] N. S. Bakhvalov, *On the optimization of methods for solving boundary value problems with boundary layers*, Zh. Vychisl. Mat. Mat. Fis., 9 (1969), pp. 841–859 (in Russian).

[6] N. M. Chadha and N. Kopteva, *Maximum norm a posteriori error estimate for a 3d singularly perturbed semilinear reaction-diffusion problem*, Adv. Comput. Math., 35 (2011), pp. 33–55.

[7] I. Cheddadi, R. Fučík, M. I. Prieto and M. Vohralík, *Guaranteed and robust a posteriori error estimates for singularly perturbed reaction diffusion equations*, M2AN Math. Model. Numer. Anal., 43 (2009), pp. 867–888.

[8] C. Clavero, J. L. Gracia and E. O'Riordan, *A parameter robust numerical method for a two dimensional reaction-diffusion problem*, Math. Comp., 74 (2005), pp. 1743–1758.

[9] A. Demlow and N. Kopteva, *Maximum-norm a posteriori error estimates for singularly perturbed elliptic reaction-diffusion problems*, Numer. Math., 133 (2016), pp. 707–742.

[10] S. Grosman, *An equilibrated residual method with a computable error approximation for a singularly perturbed reaction-diffusion problem on anisotropic finite element meshes*, M2AN Math. Model. Numer. Anal., 40 (2006), pp. 239–267.

[11] N. Kopteva *Maximum norm error analysis of a 2d singularly perturbed semilinear reaction-diffusion problem*, Math. Comp., 76 (2007), pp. 631–646.

[12] N. Kopteva, *Maximum norm a posteriori error estimate for a 2d singularly perturbed reaction-diffusion problem*, SIAM J. Numer. Anal., 46 (2008), pp. 1602–1618.

[13] N. Kopteva, *Linear finite elements may be only first-order pointwise accurate on anisotropic triangulations*, Math. Comp., 83 (2014), pp. 2061–2070.

[14] N. Kopteva, *Maximum-norm a posteriori error estimates for singularly perturbed reaction-diffusion problems on anisotropic meshes*, SIAM J. Numer. Anal., 53 (2015), pp. 2519–2544.

[15] N. Kopteva, *Energy-norm a posteriori error estimates for singularly perturbed reaction-diffusion problems on anisotropic meshes*, Numer. Math., (2017), to appear.

[16] N. Kopteva, *Energy-norm a posteriori error estimates for singularly perturbed reaction-diffusion problems on anisotropic meshes. Neumann boundary conditions*, (2016) submitted for publication, `http://www.staff.ul.ie/natalia/pubs.html`.

[17] N. Kopteva and E. O'Riordan, *Shishkin meshes in the numerical solution of singularly perturbed differential equations*, Int. J. Numer. Anal. Model., 7 (2010), pp. 393–415.

[18] G. Kunert, *An a posteriori residual error estimator for the finite element method on anisotropic tetrahedral meshes*, Numer. Math., 86 (2000), pp. 471–490.

[19] G. Kunert, *Robust a posteriori error estimation for a singularly perturbed reaction-diffusion equation on anisotropic tetrahedral meshes*, Adv. Comput. Math., 15 (2001), pp. 237–259.

[20] G. Kunert and R. Verfürth, *Edge residuals dominate a posteriori error estimates for linear finite element methods on anisotropic triangular and tetrahedral meshes*, Numer. Math., 86 (2000), pp. 283–303.

[21] H.-G. Roos, M. Stynes and L. Tobiska, *Robust Numerical Methods for Singularly Perturbed Differential Equations*, Springer, Berlin, 2008.

[22] K. G. Siebert, *An a posteriori error estimator for anisotropic refinement*, Numer. Math., 73 (1996), pp. 373–398.

[23] R. Verfürth, *Robust a posteriori error estimators for a singularly perturbed reaction-diffusion equation*, Numer. Math., 78 (1998), pp. 479–493.